Topical Review

Transient outward potassium current, 'I_{to}', phenotypes in the mammalian left ventricle: underlying molecular, cellular and biophysical mechanisms

Sangita P. Patel and Donald L. Campbell

Department of Physiology and Biophysics, University at Buffalo, State University of New York, Buffalo, NY 14214, USA

At least two functionally distinct transient outward K^+ current (I_{to}) phenotypes can exist across the free wall of the left ventricle (LV). Based upon their voltage-dependent kinetics of recovery from inactivation, these two phenotypes are designated '$I_{to,fast}$' (recovery time constants on the order of tens of milliseconds) and '$I_{to,slow}$' (recovery time constants on the order of thousands of milliseconds). Depending upon species, either $I_{to,fast}$, $I_{to,slow}$ or both current phenotypes may be expressed in the LV free wall. The expression gradients of these two I_{to} phenotypes across the LV free wall are typically heterogeneous and, depending upon species, may consist of functional *phenotypic* gradients of both $I_{to,fast}$ and $I_{to,slow}$ and/or *density* gradients of either phenotype. We review the present evidence (molecular, biophysical, electrophysiological and pharmacological) for Kv4.2/4.3 α subunits underlying LV $I_{to,fast}$ and Kv1.4 α subunits underlying LV $I_{to,slow}$ and speculate upon the potential roles of each of these currents in determining frequency-dependent action potential characteristics of LV subepicardial *versus* subendocardial myocytes in different species. We also review the possible functional implications of (i) ancillary subunits that regulate Kv1.4 and Kv4.2/4.3 (Kvβ subunits, DPPs), (ii) KChIP2 isoforms, (iii) spider toxin-mediated block of Kv4.2/4.3 (*Heteropoda* toxins, phrixotoxins), and (iv) potential mechanisms of modulation of $I_{to,fast}$ and $I_{to,slow}$ by cellular redox state, $[Ca^{2+}]_i$ and kinase-mediated phosphorylation. I_{to} phenotypic activation and state-dependent gating models and molecular structure–function relationships are also discussed.

(Resubmitted 7 March 2005; accepted after revision 13 April 2005; first published online 14 April 2005)
Corresponding author D. L. Campbell: University at Buffalo, SUNY, Department of Physiology and Biophysics, 124 Sherman Hall, Buffalo, NY 14214-3078, USA. Email: dc25@buffalo.edu

The diverse nature of cardiac myocyte action potentials arises from the non-linear and finely balanced gating characteristics of many different ionic currents (Carmeliet & Vereecke, 2002; Rudy, 2002; Nerbonne & Kass, 2003; Bondarenko *et al.* 2004; Puglisi, Wang & Bers, 2004). This electrical diversity arises from the combined effects of spatial tissue gradients of gene expression, biophysical channel gating mechanisms, second messenger systems, intracellular Ca^{2+} regulatory mechanisms and complex interactions between these multiple systems. With the advent of isolated cardiac myocyte techniques, patch clamp technology and molecular biological protocols our knowledge of many of these currents and their associated regulatory systems has significantly advanced. Nonetheless, it is sobering to realize that we are still unable to explain and quantitatively model (without making unverified assumptions) many fundamental aspects of cardiac myocyte action potentials. This is particularly true in the case of ventricular myocytes.

Due to their primary role in repolarization, and hence potential status as substrates for therapeutic interventions, extensive experimental effort has been devoted to characterizing mechanisms underlying expression and regulation of voltage-dependent potassium (Kv) channels in ventricular myocytes (Archer & Rusch, 2001; Strauss *et al.* 2001; Nerbonne & Kass, 2003). Patch clamp studies on atrial and ventricular myocytes have revealed a minimum of at least five distinct Kv-mediated native potassium current phenotypes which can be classified into two *general* functional groups: (i) 'I_{to}', rapidly activating and inactivating transient outward currents; and (ii) 'I_K' or 'delayed rectifiers'. In this review we focus on recent advances made in our understanding of the molecular, cellular and biophysical

 DOI: 10.1113/jphysiol.2005.086223

mechanisms underlying generation and regulation of I_{to} current density and phenotypic expression gradients across the well-studied left ventricular free wall. We also point out areas where there is either significant lack of understanding or major debate. This article can thus be viewed as an 'update' of the two excellent reviews on this subject that have previously appeared in this journal (Nerbonne, 2000; Sah *et al.* 2003). For readers interested in aspects of I_{to} not covered in this review the following sources may be of value: cell biology of I_{to}, Birnbaum *et al.* (2004); pathology, Chien (1999), Oudit *et al.* (2001), Nerbonne (2004) and Zicha *et al.* (2004); I_{to} expression gradients in other regions of the heart (e.g. apical–basal gradients), Brahmajothi *et al.* (1999), de Bakker & Opthof (2002) and Brunet *et al.* (2004); and the role of I_{to} phenotypes in supraventricular disturbances, Chien (1999), Van Wagoner & Nerbonne (2001) and Gussack & Antzelevitch (2003).

Cardiac ventricular I_{to} phenotypes

General characteristics

Ventricular I_{to} currents display several shared basic characteristics (Campbell *et al.* 1995; Strauss *et al.* 2001). First, all display high K^+ selectivity ($P_{Na}/P_K < 0.1$), and hence are *repolarizing* currents. Second, ventricular I_{to} currents display similar voltage-dependent gating characteristics in that all (i) activate rapidly (time constants on the order of milliseconds) in a voltage-dependent manner which is independent of previous Ca^{2+} influx, and (ii) inactivate (either as a single or mutliexponential process) with maintained depolarization (time constants on the order of tens to hundreds of milliseconds). All I_{to} currents are thus modulators of both early phase 1 repolarization and the excitation–contraction (EC) coupling cycle (Campbell *et al.* 1995; Bers, 2001; Oudit *et al.* 2001; Nerbonne & Kass, 2003; Sah *et al.* 2003) (Fig. 1).

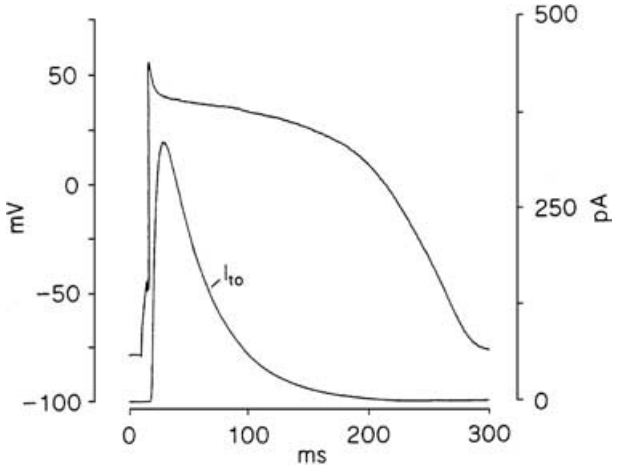

Figure 1. Conventional whole cell patch clamp view of I_{to}: theoretically predicted kinetic behaviour of $I_{to,fast}$ during a ventricular action potential
The illustrated action potential was recorded from a ferret right ventricular myocyte (22°C), while the corresponding $I_{to,fast}$ waveform was generated using the recorded action potential waveform as the voltage 'driving function' for the $I_{to,fast}$ gating equations developed by Campbell *et al.* (1993*a*,*b*). Such predicted behaviour may only reflect the kinetics of $I_{to,fast}$ under 'basal' conditions, i.e. in the absence of normal $[Ca^{2+}]_i$ transients and minimal kinase-mediated regulation. Figure reproduced from Campbell *et al.* (1995) with permission from Elsevier.

Prominent I_{to} currents have been recorded in ventricular myocytes isolated from the hearts of many species, including mice, rats, rabbits, cows, cats, dogs, ferrets and humans (Campbell *et al.* 1995; Strauss *et al.* 2001; Carmeliet & Vereecke, 2002; Nerbonne & Kass, 2003; Nerbonne, 2004). One notable exception is the guinea pig, where I_{to} is very small or absent (Varro *et al.* 1993; Nerbonne & Kass, 2003; Zicha *et al.* 2003). Thus, in the vast majority of species I_{to} is a prominent current in ventricular myocytes. The term 'I_{to}' has therefore become synonymous with any rapidly activating and inactivating ventricular K^+ current. However, depending upon species and anatomical region, there are at least two distinct I_{to} *phenotypes* that can be distinguished based upon molecular, biophysical and pharmacological properties. For the left ventricular (LV) free wall, depending upon species, two I_{to} *expression gradients* exist: (i) a gradient of two *functionally* distinct I_{to} phenotypes; and (ii) a gradient in peak current density (pA/pF) of a single functional I_{to} phenotype. In many species, including humans, both gradient types are simultaneously expressed.

Functionally distinct I_{to} phenotypic gradients

In the LV free walls of rats, ferrets and humans an expression gradient of at least two major functionally distinct I_{to} phenotypes exists (e.g. Shimoni *et al.* 1995; Näbauer *et al.* 1996; Brahmajothi *et al.* 1999). Multiple I_{to} phenotypes are also expressed in different anatomical regions of the mouse heart (e.g. Xu *et al.* 1999; Guo *et al.* 1999; Brunet *et al.* 2004).

Inactivation/recovery kinetics. The most distinguishing biophysical characteristics for the two major ventricular I_{to} phenotypes are differences in the kinetics of inactivation and, in particular, the kinetics of recovery from inactivation ('recovery'). In LV subepicardial (LV epi) myocytes of humans and ferrets inactivation of native I_{to} is approximated as a single exponential process, with time constants of ∼30–100 ms (Näbauer *et al.* 1996; Brahmajothi *et al.* 1999) (Fig. 2). Inactivation time constants become voltage independent at depolarized potentials, suggesting a voltage-independent rate-limiting step. Voltage-dependent recovery kinetics (∼ −100 to −60 mV) of this I_{to} phenotype are fast, with time constants

on the order of ~20–100 ms (Campbell *et al.* 1995; Strauss *et al.* 2001; Nerbonne & Kass, 2003). Because of these fast recovery kinetics, rapid repetitive voltage clamp pulses result in very little to no cumulative inactivation (Aldrich, 1981). This I_{to} phenotype is therefore designated '$I_{to,fast}$', with 'fast' describing the recovery kinetics.

In many species a second I_{to} phenotype has been identified which inactivates as a distinct double exponential process. The rapid time constant of inactivation has values similar to those displayed by $I_{to,fast}$, while the slower time constant is on the order of hundreds of milliseconds. However, this I_{to} phenotype is truly distinguished by its very slow recovery kinetics, with voltage-dependent time constants on the order of *seconds* (e.g. Giles & Imaizumi, 1988; Clark *et al.* 1988; Näbauer *et al.* 1996; Brahmajothi *et al.* 1999; Nerbonne & Kass, 2003). Another unique kinetic characteristic of this current is development of prominent cumulative inactivation during rapid repetitive voltage-clamp pulses (Aldrich, 1981; Giles & Imaizumi, 1988; Näbauer *et al.* 1996; Brahmajothi *et al.* 1999; Nerbonne & Kass, 2003) (Fig. 2). This cumulatively inactivating I_{to} phenotype is therefore designated '$I_{to,slow}$', with 'slow' describing the recovery kinetics.

Activation/deactivation kinetics. Limited quantitative data exist on the voltage-dependent activation and deactivation kinetics of $I_{to,fast}$ and $I_{to,slow}$ in LV myocytes. The most detailed analysis has been conducted on $I_{to,fast}$ in ferret right ventricular (RV) myocytes (Campbell *et al.* 1993*b*), which demonstrated that voltage-dependent activation kinetics were sigmoidal. Sigmoidicity of activation and subsequent inactivation (well-approximated as a single exponential) could be described with a Hodgkin-Huxley-like 'a^3i' formulation (Hodgkin & Huxley, 1952). While the HH-like kinetic model developed from this analysis was able to successfully reproduce many aspects of RV $I_{to,fast}$ gating (Campbell *et al.* 1993*a*,*b*), it is unlikely that its basic assumptions, particularly the assumption of independence of activation

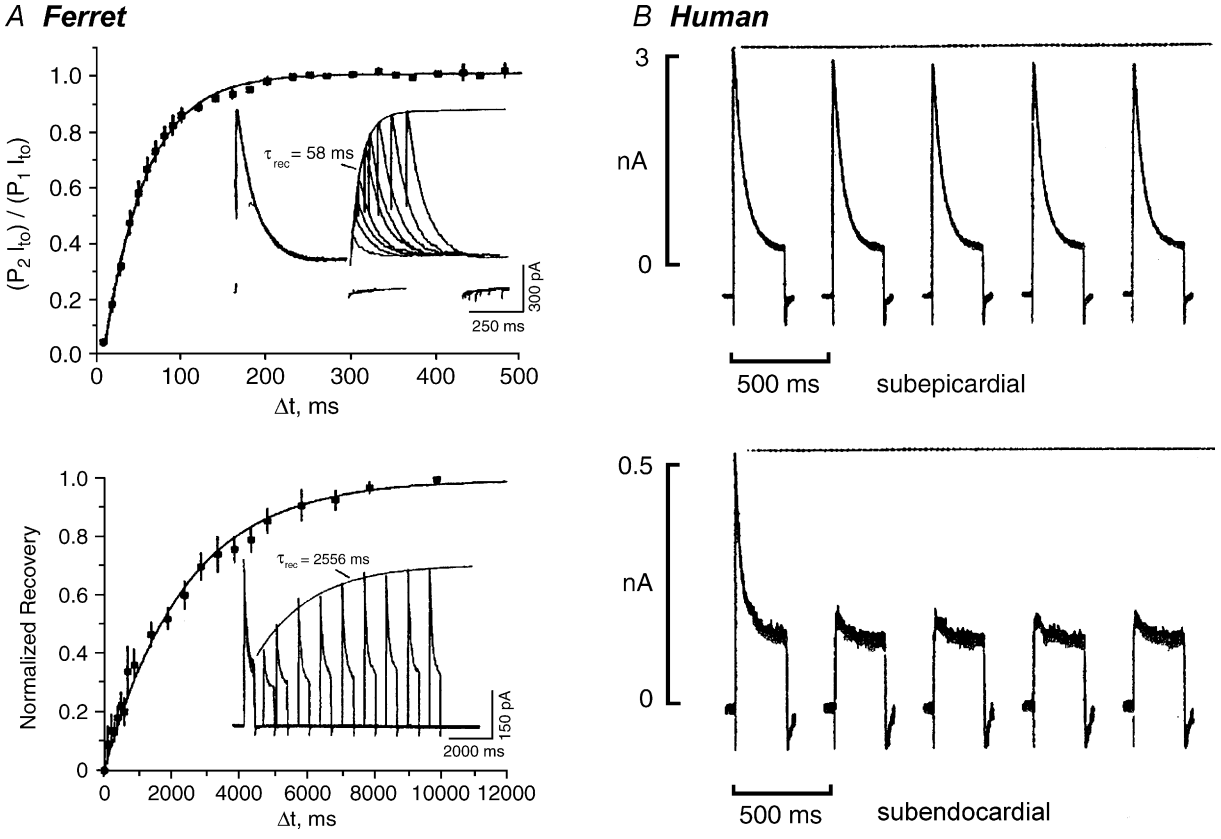

Figure 2. Distinct recovery kinetics and frequency-dependent inactivation characteristics of $I_{to,fast}$ and $I_{to,slow}$

A, recovery waveforms (22°C, HP = −70 mV) for ferret LV epi myoctye $I_{to,fast}$ (upper panel) and LV endo myocyte $I_{to,slow}$ (lower panel). *B*, frequency-dependent recovery characteristics of human LV epi myocyte $I_{to,fast}$ (upper panel; minimal cumulative inactivation) and LV endo myocyte $I_{to,slow}$ (lower panel; marked cumulative inactivation). From HP = −80 mV currents were repetitively generated (2 Hz, 250 ms clamp step pulses to +40 mV). Data from: ferret, modified from Brahmajothi *et al.* (1999) by copyright permission of The Rockefeller University Press; human, Näbauer *et al.* (1996) with permission of Lippincott Williams & Wilkins.

and inactivation, are correct at the molecular level (for further discussion see: Yellen, 1998, 2002; Bezanilla, 2000; Hille, 2001*a*; Wang *et al.* 2004).

Pharmacological properties of $I_{to,fast}$ *versus* $I_{to,slow}$: 4-aminopyridine and spider toxins. *4-Aminopyridine.* While 4-aminopyridine (4-AP) is non-specific in that it blocks both $I_{to,fast}$ and $I_{to,slow}$, the underlying mechanisms are quite distinct. Block of $I_{to,slow}$ displays classic characteristics of open-state block: minimal tonic block, apparent acceleration of inactivation, and use dependence (Campbell *et al.* 1993*a*; Hille, 2001*b*). In contrast, 4-AP block of $I_{to,fast}$ occurs through closed-state binding and displays 'reverse use dependence'. These properties have been most thoroughly analysed for ferret RV $I_{to,fast}$ (Campbell *et al.* 1993*a*,*b*). Closed-state block is manifested not only by a reduction in peak $I_{to,fast}$ amplitude but also by a slowing in the kinetics of activation and inactivation, 'crossover' of the partially blocked current with the unblocked current, relief of block during repetitive voltage clamp pulses, and redevelopment of block upon repolarization (Fig. 3).

Spider toxins. Heteropoda toxins (HPTXs 1–3) are 30–33 amino acid peptides isolated from the venom of the Malaysian spider *Heteropoda venatoria* (Sanguineti *et al.* 1997; Bernard *et al.* 2000; amino acid sequences illustrated in Fig. 14*A*). HPTX2 at 150 nM has no effect on $I_{to,slow}$ in ferret LV endo myocytes but inhibits $I_{to,fast}$ in LV epi myocytes (Brahmajothi *et al.* 1999). Inhibition is voltage dependent and relieved with depolarization (Fig. 4*A*). The apparent K_d for inhibition ranges from 105 nM at +20 mV to 559 nM at +70 mV. HPTXs also block $I_{to,fast}$ but not $I_{to,slow}$ in mouse ventricular myocytes (Xu *et al.* 1999; Guo *et al.* 1999). Consistent with these results, 30 nM HPTX2 lengthens action potentials in rat ventricular myocytes (Sanguinetti *et al.* 1997; Fig. 4*B*).

Another family of spider toxins that selectively interact with $I_{to,fast}$ are the phrixotoxins (PaTXs; Diochot *et al.* 1999). PaTXs are 29–31 amino acid peptides isolated from the venom of the Chilean fire tarantula, *Phrixotrichus aurata* (amino acid sequences given in Fig. 14*A*). When injected into mice, PaTX1 produces varying degrees of atrioventricular block, premature ventricular beats, tachycardia and prolongation of the QT interval. However, the extent to which these effects are due to inhibition of LV $I_{to,fast}$ *versus* $I_{to,fast}$ in other tissues (particularly neurones) is unclear.

I_{to} density gradients

In most species there is a marked peak current *density* gradient (pA/pF) for I_{to} in LV epi *versus* LV endo myocytes.

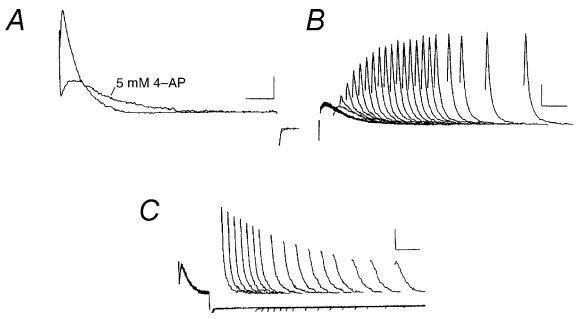

Figure 3. 4-Aminopyridine: closed-state 'reverse use-dependent' block of native $I_{to,fast}$ in ferret right ventricular myocytes
A, steady-state block of $I_{to,fast}$ elicited at +50 mV by 5 mM 4-AP. 4-AP slows both activation and inactivation kinetics, producing a crossover in the current waveforms. *B*, relief of 4-AP block with increasing depolarizing pulse duration. Currents were elicited during the P2 pulse to +50 mV as the duration of the preceding P1 pulse (500 ms, +50 mV) was progressively increased. *C*, relief of block and subsequent reassociation of 4-AP (10 mM) during a conventional 500 ms P1–P2 double pulse protocol to +50 mV (HP = −60 mV). Note relief of block during the P1 pulse, and reassociation of 4-AP to channel closed-states as the interpulse interval duration is increased. Data from Campbell *et al.* (1993*a*) by copyright permission of The Rockefeller University Press; protocol details given therein.

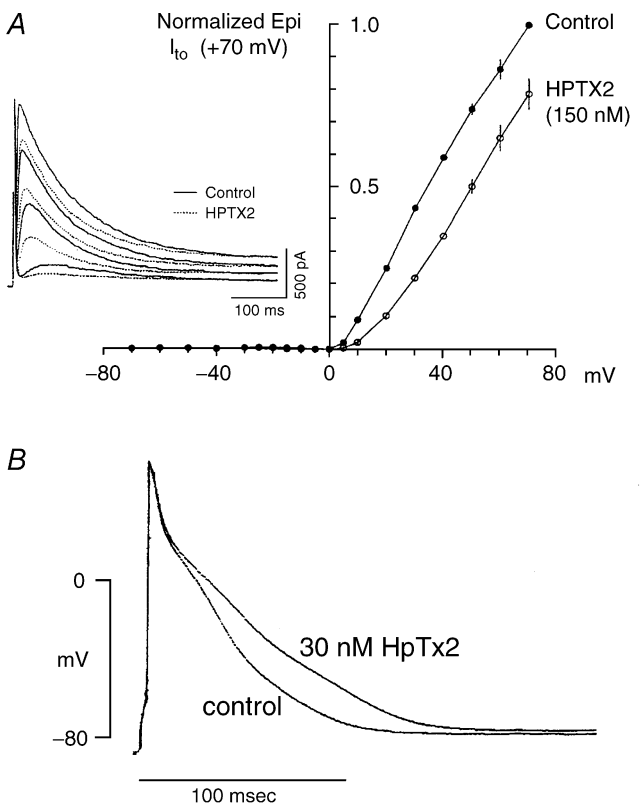

Figure 4. Spider toxins: HPTX2 selectively blocks native $I_{to,fast}$ in a voltage-dependent manner
A, block of ferret LV epi myocyte $I_{to,fast}$ by 150 nM HPTX2. Inset: $I_{to,fast}$ in control solution (continuous lines) and after extracellular application of 150 nM HPTX2 (dashed lines). *B*, effect of 30 nM HPTX2 on the action potential recorded from a rat ventricular myocyte. Data for ferret from Brahmajothi *et al.* (1999) by copyright permission of The Rockefeller University Press; for rat reproduced with permission from Sanguinetti *et al.* (1997).

Such density gradients have been reported for rat, rabbit, dog, ferret and human (Strauss *et al.* 2001; Nerbonne & Kass, 2003). However, the *phenotypic* nature of these density gradients is species specific (Fig. 5). For example, in ferret and human phenotypic I_{to} gradients are present, with $I_{to,fast}$ being prominently expressed in LV epi myocytes and $I_{to,slow}$ in LV endo myocytes (Näbauer *et al.* 1996; Brahmajothi *et al.* 1999). In both species the density of LV epi $I_{to,fast}$ is ∼4–5 times greater than LV endo $I_{to,slow}$. In contrast, in dog there is only a density gradient of $I_{to,fast}$ (∼4–5 times higher in LV epi than LV endo myocytes; Liu *et al.* 1993; Antzelevitch, Zygmunt & Dumaine, 2003), while in rabbit $I_{to,slow}$ density is higher in LV epi than LV endo myocytes (Fedida & Giles, 1991).

Molecular basis of ventricular I_{to} phenotypes

The three candidate K^+ channel clones for generating distinct I_{to} phenotypes are Kv1.4, Kv4.2 and Kv4.3 (Nerbonne, 2000; Archer & Rusch, 2001; Oudit *et al.* 2001; Strauss *et al.* 2001; Sah *et al.* 2003; Nerbonne & Kass, 2003). These clones have been assigned to native I_{to} phenotypes recorded in LV myocytes based upon their electrophysiological characteristics, sensitivity to HPTXs/PaTXs and 4-AP, molecular expression patterns, and properties when manipulated in transgenic mice.

Kv1.4. Kv1.4 α subunits (Fig. 6) display: (i) rapid sigmoidal activation kinetics; (ii) biexponential inactivation kinetics; (iii) very slow kinetics of recovery

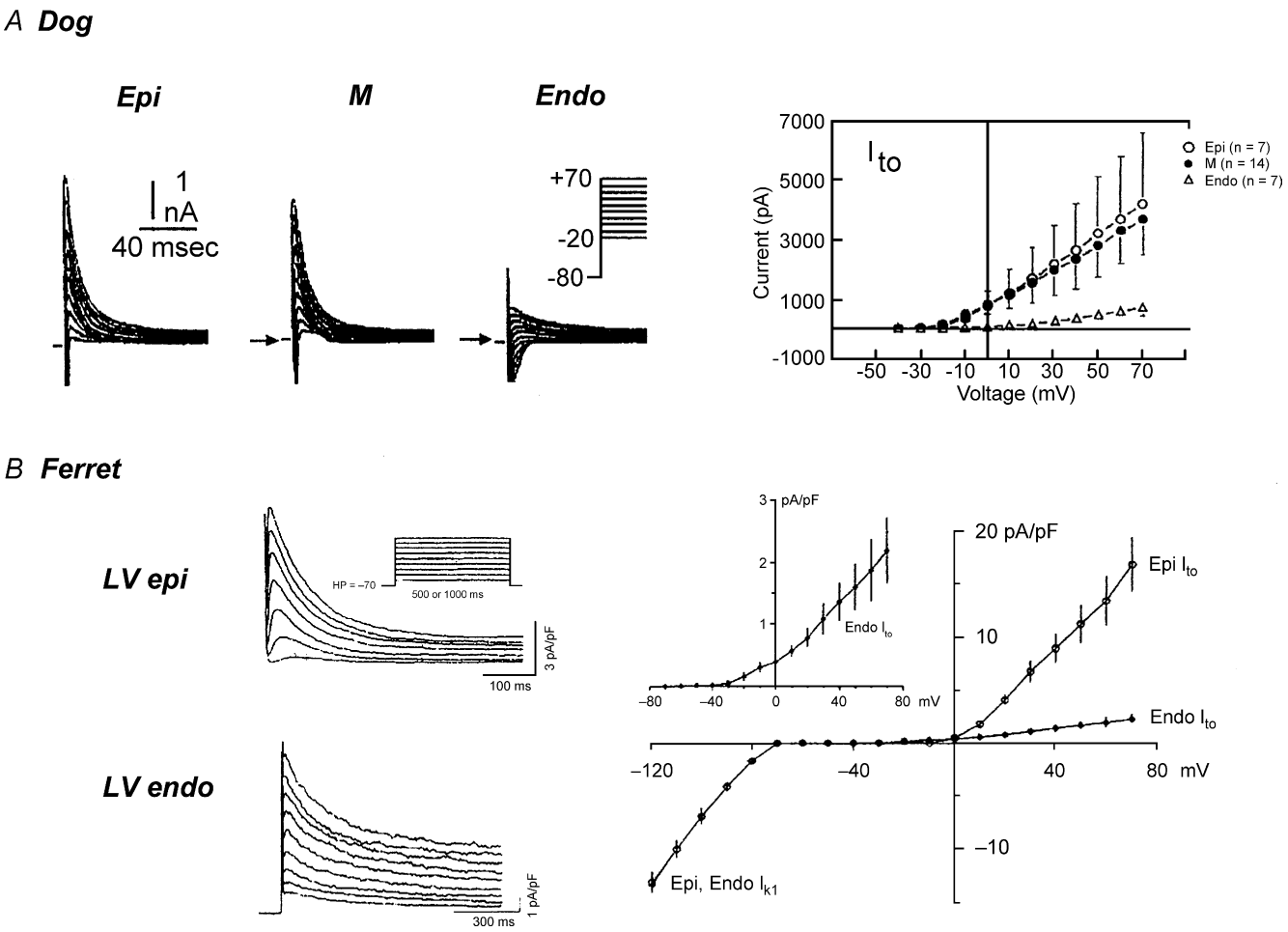

Figure 5. Comparative I_{to} cellular physiology
Representative LV free wall I_{to} phenotypic and density gradients. Peak I_{to} current density–voltage relations in dog (*A*) and ferret (*B*) LV epi and LV endo myocytes. Also illustrated in *A* is the peak current–voltage relationship obtained in dog midventricular M-cells. Both species display I_{to} density gradients. Currents generated as follows: dog, HP = −80 mV, pulses from −20 to +70 mV (overlapping inward currents not blocked); ferret, HP = −70 mV, pulses from 0 to +60 mV (LV epi) and −10 to +70 mV (LV endo). Data from: dog, Liu *et al.* (1993) by permission of Lippincott Williams & Wilkins; ferret, Brahmajothi *et al.* (1999) by copyright permission of The Rockefeller University Press.

(time constants on the order of seconds); (iv) cumulative inactivation during repetitive voltage clamp pulses; (v) open-state block by 4-AP (Fig. 7); and (vi) insensitivity to HPTXs, PaTXs and flecanide (Tseng-Crank *et al.* 1990; Tamkun *et al.* 1991; Po *et al.* 1992; Comer *et al.* 1994; Rasmusson *et al.* 1995*a*,*b*, 1998; Sanguinetti *et al.* 1997; Roeper *et al.* 1997; McKinnon, 1999; Petersen & Nerbonne, 1999; Robertson, 2001; Oudit *et al.* 2001; Jiang *et al.* 2003*a*; Li *et al.* 2003; Nerbonne & Kass, 2003; Bett & Rasmusson, 2004). Hence, the biophysical, kinetic and pharmacological characteristics of Kv1.4-mediated currents are very similar to those displayed by native LV $I_{to,slow}$.

Very strong evidence for Kv1.4 underlying the LV $I_{to,slow}$ phenotype comes from elegant studies on transgenic mice which have shown that interventricular myocytes with a targeted deletion of Kv1.4 display complete loss of $I_{to,slow}$ but not $I_{to,fast}$. In contrast, mice expressing a truncated Kv4.2 display reduced $I_{to,fast}$ expression, and a Kv4.2 pore mutant (Kv4.2W62F) which acts as a dominant negative results in selective loss of $I_{to,fast}$ (Barry *et al.* 1998; Guo *et al.* 1999; Xu *et al.* 1999; Wickenden *et al.* 1999). In these mice with deleted/reduced $I_{to,fast}$, $I_{to,slow}$ becomes more prominent in the LV, indicating that the two current phenotypes are regulated by different potassium channels. Finally, in ferret both the phenotypic and density gradients of $I_{to,slow}$ closely parallel the Kv1.4 protein expression gradient, with both $I_{to,slow}$ and Kv1.4 being highly expressed in the LV endo but not LV epi or right ventricle (Brahmajothi *et al.* 1999).

Kv4.2 and Kv4.3. Kv4.2 and Kv4.3 α subunits (Fig. 6) display: (i) rapid sigmoidal activation kinetics; (ii) multiexponential inactivation kinetics; (iii) rapid kinetics of recovery (time constants on the order of 10 to hundreds of milliseconds); (iv) little to no cumulative inactivation during repetitive voltage clamp pulses; (v) closed-state, reverse use-dependent block by 4-AP (Fig. 7); and (vi) sensitivity to HPTXs, PaTXs and flecanide (Serodio *et al.* 1996; Tseng *et al.* 1996; Dixon *et al.* 1996; Yeola & Snyders, 1997; Sanguinetti *et al.* 1997; Kääb *et al.* 1998; Favre *et al.* 1999; Franqueza *et al.* 1999; Jerng *et al.* 1999; Nerbonne, 2000; Archer & Rusch, 2001; Robertson, 2001; Strauss *et al.* 2001; Beck & Corvarrubias, 2001; Oudit *et al.* 2001; Bähring *et al.* 2001*a*,*b*; Beck *et al.* 2002; Guo *et al.* 2002*a*; Patel *et al.* 2002*a*,*b*, 2004; Wang *et al.* 2002, 2004; Shahidulla & Covarrubias, 2003; Sah *et al.* 2003; Nerbonne & Kass, 2003; Gebauer *et al.* 2004; Hatano *et al.* 2004; Jerng, Qian & Pfaffinger, 2004).

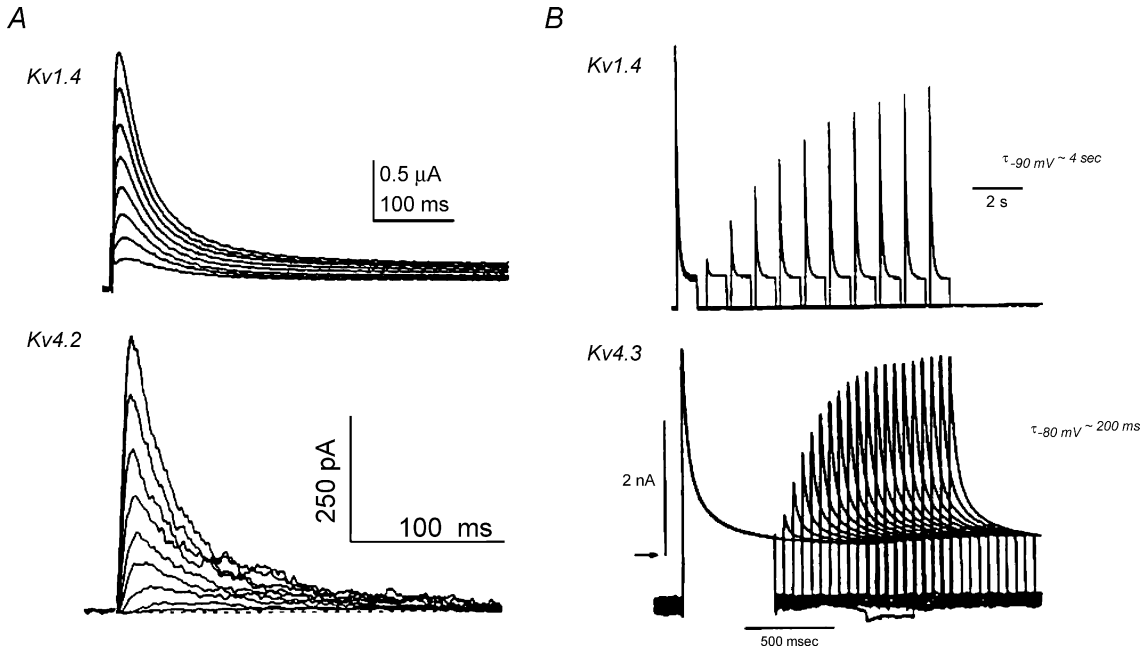

Figure 6. Currents generated by heterologously expressed Kv1.4 and Kv4.2/4.3
A, while both Kv1.4 and Kv4.2/4.3 (Kv4.2 illustrated) give rise to transient outward K^+ currents at depolarized potentials that resemble native LV I_{to} phenotypes, there is approximately an order of magnitude difference in their kinetics of recovery. *B*, Kv4.3 recovers with time constants on the order of hundreds of milliseconds, while Kv1.4 recovers with time constants on the order of seconds and displays marked cumulative inactivation during repetitive voltage clamp pulses. Data from: *A*, Kv1.4, Comer *et al.* (1994) (used with permission from the American Physiological Society); Kv4.2, Yeola & Snyders (1997) with permission from the European Society of Cardiology; *B*, Kv1.4, Rasmusson *et al.* (1995*b*); Kv4.3, Favre *et al.* (1999) with permission from the European Society of Cardiology.

Similar to their effects on native LV epi $I_{to,fast}$, HPTXs and PaTXs both inhibit Kv4.2/4.3 in a voltage-dependent manner, with inhibition relieved with progressive depolarization (Sanguinetti *et al.* 1997; Brahmajothi *et al.* 1999). Assuming a single binding site, apparent K_d values for HPTX2 inhibition (100 nM) of peak Kv4.2 current range from 35 nM at +20 mV to 138 nM at +50 mV (Sanguinetti *et al.* 1997). Similarly, percentage inhibition of peak Kv4.3 current by PaTX1 (100 nM) ranges from ∼50–60% at −30 mV to ∼20% at +50 mV (Diochot *et al.* 1999).

While pharmacological properties of $I_{to,fast}$ are mimicked by Kv4.2/4.3, many physiologically important kinetic properties of $I_{to,fast}$ are only partially reconstituted by these clones. In particular, while recovery kinetics of Kv4.2/4.3 are ∼10-fold faster than those of both Kv1.4 and native LV $I_{to,slow}$, they are still ∼5-fold slower than native LV $I_{to,fast}$. This suggests involvement of additional regulatory subunits in LV myocytes. Also, both Kv4.2 and Kv4.3 display little to no cumulative inactivation, either when expressed alone or in the presence of regulatory subunits (discussed below).

Regulatory subunits

Kv1.4-mediated $I_{to,slow}$. While the kinetic properties of Kv1.4 α subunits expressed alone closely reproduce the properties of native 'basal' LV $I_{to,slow}$, Kv1.4 α subunits are also subject to regulation by β subunits. Four homologous β subunits have been identified to date (Kvβ1–β4); however, only Kvβ1, β2 and β3 interact with Kv1 channels. Among these, Kvβ1 (alternative splice variants β1.2 and β1.3) and Kvβ2 RNA are expressed in the heart (e.g. Morales *et al.* 1995; Deal *et al.* 1996). These subunits lack transmembrane domains and thus are of putative intracellular topology. Their regulatory properties include chaperone effects, modulation of voltage dependence and alteration of inactivation kinetics (Nerbonne & Kass, 2003). For example, Kvβ1.3 accelerates both the fast and slow components of inactivation, promotes the slower component of inactivation and slows recovery of Kv1.4 (Morales *et al.* 1995; Castellino *et al.* 1995; Fig. 8*A*). β subunits can also act as 'inactivation balls' – coexpression with N-terminus-deleted Kv1.4 channels that lack fast N-type inactivation results in reestablishment of inactivation (Fig. 8*B*).

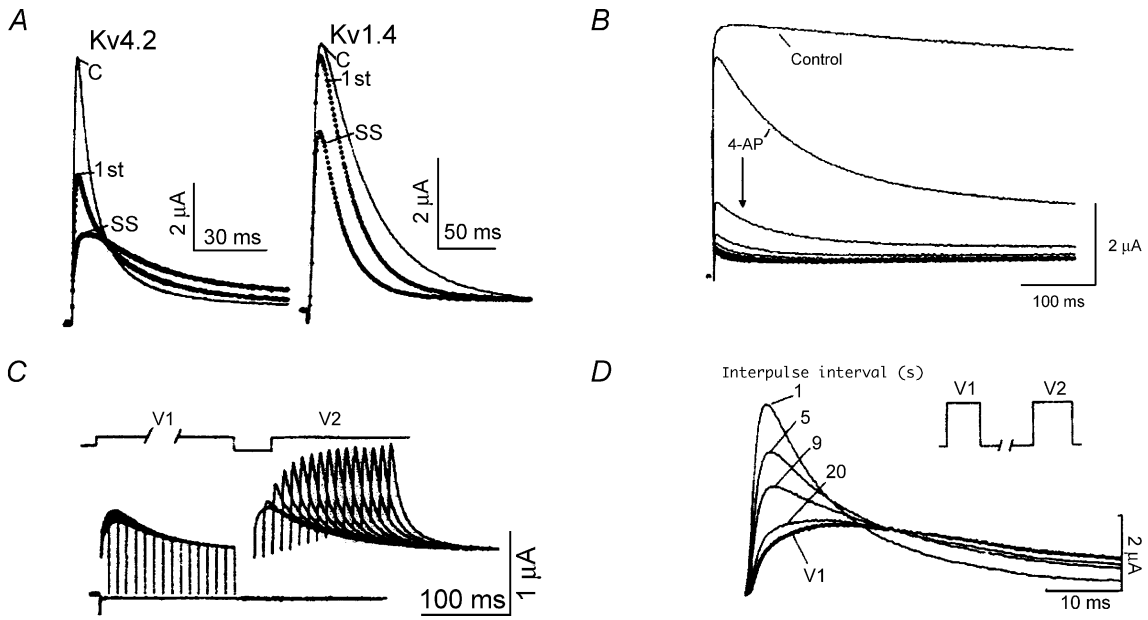

Figure 7. 4-Aminopyridine: Kv1.4 *versus* Kv4.2 – open-state *versus* closed-state blocking effects
A, effect of 4-AP on Kv4.2 (20 mM; compare to Fig. 3*A*) and Kv1.4 (1 mM) peak currents and kinetics. Kv4.2, 250 ms pulses to +60 mV, Kv1.4, 500 ms pulses to +20 mV, both elicited from HP = −80 mV and frequency of 1 pulse min^{-1}. Illustrated are currents before application of 4-AP (C), during the first pulse after application of 4-AP (1st) and steady-state currents (SS). *B*, effects of 10 mM 4-AP on the ferret Kv1.4 N-terminal deletion mutant NCO (removes rapid N-type inactivation). Step pulses of 500 ms to +50 mV, HP = −90 mV, frequency 0.1 Hz. Note both classic use dependence and development of apparent inactivation-like behaviour in the presence of 4-AP. *C*, time dependence of 4-AP (10 mM) unblock of Kv4.2 at depolarized potentials. Pulses V_1 and V_2 were both applied to +60 mV at a frequency of 1 pulse/2 min (HP = −80 mV), while the V_1 duration was progressively increased. Compare to Fig. 3*B*. *D*, reassociation of 4-AP to Kv4.2 closed states after a depolarizing pulse. V_1 and V_2 both to +60 mV. Corresponding V_2 currents overlaid for the indicated interpulse intervals in seconds. Compare to Fig. 3*C*. Data for Kv4.2 reproduced with permission from Tseng *et al.* (1996); for Kv1.4 from Rasmusson *et al.* (1995*b*).

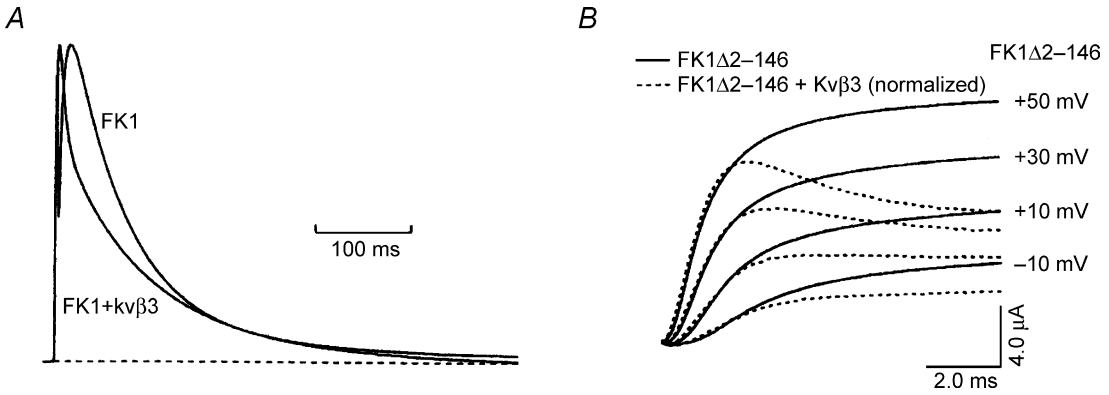

Figure 8. Representative effects of Kvβ subunits on Kv1.4 inactivation kinetics
A, effects of Kvβ3 on ferret Kv1.4 (originally designated FK1 by Comer *et al.* 1994). Depolarizing voltage clamp pulses to +50 mV from HP = −90 mV. Kvβ3 induced both a rapid early phase of inactivation and a smaller, slower phase of inactivation. *B*, in the absence of rapid N-type inactivation (N-terminal amino acids 2–146 deleted from Kv1.4 (FK1Δ2–146)) Kvβ3 can act as a partial 'inactivation ball' with minimal effects on activation kinetics. Data in *A* from Morales *et al.* (1995) reproduced with permission of the American Society for Biochemistry & Molecular Biology; data in *B* from Castellino *et al.* (1995), used with permission from the American Physiological Society.

Kv1-interacting β subunits are non-enzymatic homologues of aldo-keto reductases (McCormack & McCormack, 1994; Gulbis *et al.* 1999; Campomanes *et al.* 2002). It is thus possible that β subunits may impart selective cellular redox-state sensitivity to LV $I_{to,slow}$. For example, in the LV free walls of ferrets and humans the expression gradients of Type III nitric oxide synthase (eNOS) and sarcolemmal bound superoxide dismutase (ECSOD) closely parallel the phenotypic I_{to} gradients (Näbauer *et al.* 1996; Brahmajothi *et al.* 1999) (Fig. 9). But it is unknown if expression gradients of Kvβ subunits also parallel those of eNOS/ECSOD

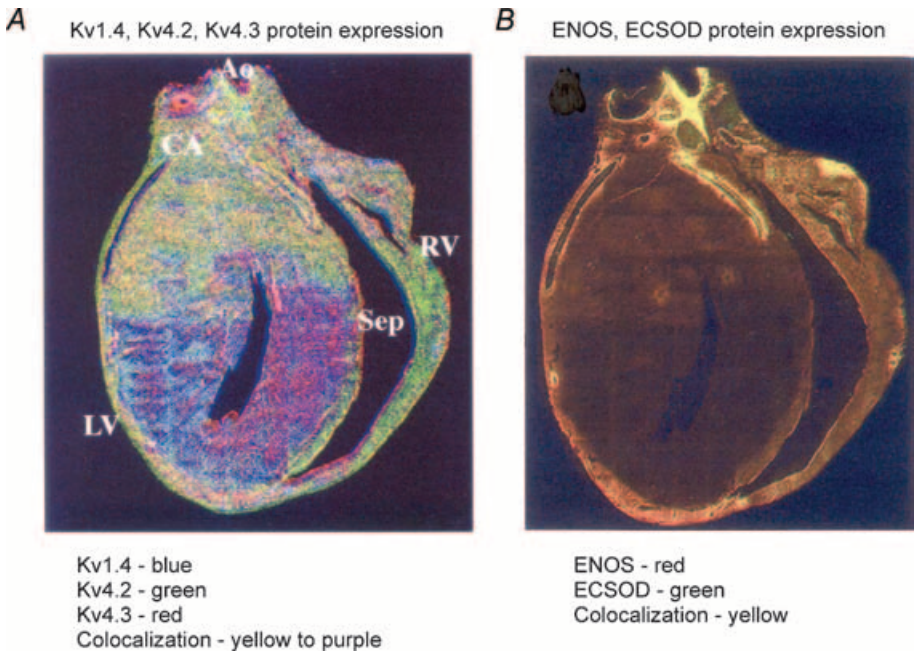

Figure 9. Immunofluorescent localization: overlap of expression gradients of I_{to} α subunit proteins and eNOS and ECSOD proteins in ferret heart
A, expression gradients of Kv1.4 (blue), Kv4.2 (green) and Kv4.3 (red). CA, coronary artery; Ao, aorta; Sep, septum; RV, right ventricle; LV, left ventricle. In addition to the transmural LV free wall gradients also note the apical to basal gradients. *B*, expression gradients of eNOS (red) and ECSOD (green). Data from: I_{to} α subunits, Brahmajothi *et al.* (1999) by copyright permission of The Rockefeller University Press; eNOS and ECSOD, Brahmajothi & Campbell (1999) by permission of Lippincott Williams & Wilkins.

and the two I_{to} phenotypes. If this turns out to be the case, could Kvβ subunits provide a 'missing link' for selective O_2, NO- and/or redox-related modulation of LV repolarization and EC-coupling characteristics under normal and pathological conditions (Ruppersberg *et al.* 1991*b*; Campbell *et al.* 1996; Perez-Garcia *et al.* 1999; Brahmajothi & Campbell, 1999; Holmqvist *et al.* 2001)?

Kv4.2/4.3-mediated $I_{to,fast}$. *Kv Channel Interacting Proteins.* The discrepancy between recovery kinetics of Kv4.2/4.3 and native LV epi $I_{to,fast}$ suggests the presence of additional ancillary subunits involved in regulation of $I_{to,fast}$ gating kinetics. The *K*v *Ch*annel *I*nteracting *P*roteins (KChIPs) are one such family of ancillary subunits. KChIPS are members of the neuronal calcium sensors subfamily of Ca^{2+}-binding proteins typically characterized by four Ca^{2+}-binding EF-hands (Linse & Forsén, 1995; Nef, 1996; Ikura, 1996). Additional members of this family include DREAM (calsenilin), frequenin (neuronal calcium sensor-1) and hippocalcin.

An *et al.* (2000) originally identified three KChIPs (KChIP1, 2 and 3) encoded by different genes. Each KChIP has a distinct N-terminus, but ~70% amino acid identity over the C-terminus. The C-termini of these KChIPs also share significant homology with frequenin and hippocalcin. Since the original work of An *et al.* (2000), four KChIP genes have now been identified (KChIP1–4). Members of the KChIP2 family are the predominant isoforms expressed in ventricular muscle. To date, at least eight KChIP2 isoforms have been identified and characterized (An *et al.* 2000; Kuo *et al.* 2001; Ohya *et al.* 2001; Bähring *et al.* 2001*a*; Rosati *et al.* 2001, 2003; Decher *et al.* 2001, 2004; Patel *et al.* 2002*a*,*b*; Hatano *et al.* 2004).

KChIPs bind to the N-terminus of Kv4 channels with a stoichiometry of 1 KChIP per Kv4 α subunit (4 KChIPs per tetrameric channel complex; Kim *et al.* 2003). Biophysically, most KChIP2 isoforms influence Kv4 channels by (Fig. 10): (i) slowing the kinetics of the fast component of inactivation; (ii) accelerating the kinetics of the slow component of inactivation; (iii) favouring gating shifts such that the slow component of inactivation becomes dominant at depolarized potentials; and (iv) accelerating the kinetics of recovery to rates similar to those of native LV epi $I_{to,fast}$ (An *et al.* 2000; Kuo *et al.* 2001; Bähring *et al.* 2001*a*; Rosati *et al.* 2001, 2003; Decher

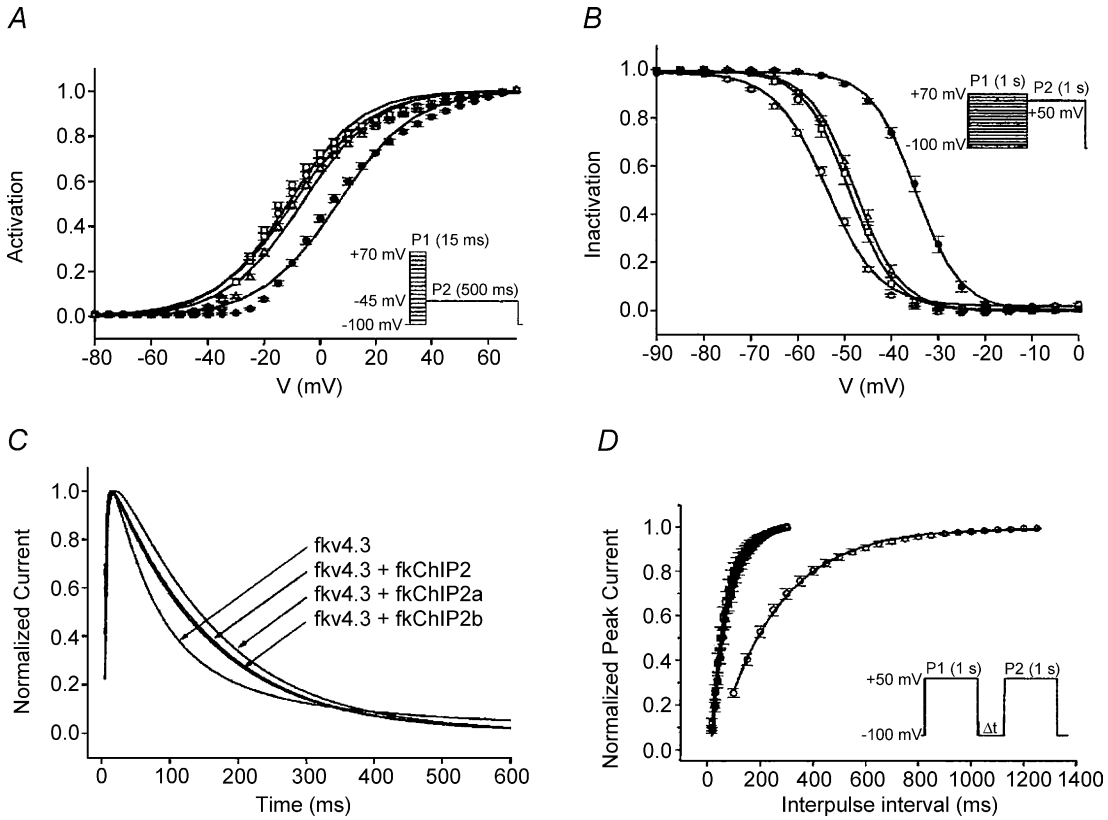

Figure 10. 'Conventional' regulatory effects of KChIP isoforms 2 (□), 2a (●) and 2b (△) on Kv4.3 (○) gating characteristics
A, steady-state activation relationships. *B*, inactivation relationships. *C*, inactivation kinetics at +50 mV (peak currents normalized for comparison). *D*, recovery kinetics at HP = −100 mV. Data from Patel *et al.* (2002*a*).

et al. 2001, 2004; Patel *et al.* 2002*a*,*b*, 2004). In contrast to their regulatory effects on inactivation and recovery, KChIP2 isoforms have minimal effects on the kinetics or voltage dependence of Kv4 channel activation; however, they significantly accelerate deactivation kinetics (Patel *et al.* 2004).

KChIPs also promote Kv4 channel cell surface expression, functionally manifested by an increase in peak current amplitude/density with no change in single channel conductance (Bähring *et al.* 2001*a*; Beck *et al.* 2002; refer to Birnbaum *et al.* (2004) for further discussion of KChIP-related trafficking effects). This function of KChIP2 is dramatically illustrated by the absence of $I_{to,fast}$ in mice lacking the KChIP2 gene (Kuo *et al.* 2001).

While it is assumed that EF-hands in KChIPs play important regulatory roles, little is actually understood about how KChIPs and Ca^{2+} binding to them regulate Kv4.2/4.3 gating. In KChIP1, EF-hands 1 and 2 are non-canonical and degenerate (Zhou *et al.* 2004; see Fig. 15*E*), leaving EF-hands 3 and 4 as the potential sensors/transducers of Ca^{2+}-dependent regulation. This is further supported by ANS fluorescence studies of the metal binding properties of KChIP1, which suggest that EF-hand 4 has the greatest structural and functional importance (Chang *et al.* 2003).

Currently, no quantitative measurements of Ca^{2+}-binding affinities of EF-hands in KChIP2 isoforms are available. However, DREAM (KChIP3) has a high affinity Ca^{2+}-binding site (K_d $\sim 6 \times 10^{-7}$ M) located in either EF hand 3 or 4, and Ca^{2+} binding to this site produces significant changes in secondary structure (Craig *et al.* 2002). If the K_d of DREAM is similar to KChIP2 isoforms, then cyclical changes in $[Ca^{2+}]_i$ that occur during a normal LV myocyte action potential could dynamically alter Kv4.2/4.3 gating kinetics (Patel *et al.* 2002*b*, 2004).

The functional role of EF-hand 4 of the KChIP2 isoforms has been studied utilizing KChIP2d, which corresponds to the last 70 C-terminal amino acids of the other larger isoforms, and thus contains only the fourth EF-hand (Patel *et al.* 2002*b*, 2004). Nonetheless, KChIP2d retains both Ca^{2+}-dependent and Ca^{2+}-independent functional effects on Kv4.3 gating kinetics. Ca^{2+} dependency manifests itself in the promotion of the slower component of inactivation, while the reduction of the faster component of inactivation and acceleration of recovery are both Ca^{2+} independent (Patel *et al.* 2002*b*). The presence of EF-hand 4 alone is thus sufficient for mediating the Ca^{2+}-dependent effects on Kv4.3 gating. The magnitude of these Ca^{2+}-dependent effects is greater in the presence of KChIP2b with its four EF-hands.

Other regions of KChIP molecules that regulate specific Kv.4 functions have also been studied. Truncation of both KChIPs 1 and 2 to the highly conserved 185 amino acid C-terminus sequence (KChIP1ΔN2-31, KChIP2ΔN2-67) resulted in no significant loss of regulatory function on Kv4.2 kinetics (An *et al.* 2000), results consistent with the regulatory effects displayed by KChIP2d (Patel *et al.* 2002*b*, 2004). Analysis of the effects of various KChIP2 chimaeric constructs (specific regions swapped between neuronal Ca^{2+} sensor-1 and KChIP2) on Kv4.3 gating indicated three important regions of KChIP2: (i) the linker between EF-hands 1 and 2; (ii) the linker between EF-hands 3 and 4; and (iii) the C-terminal peptide after EF-hand 4 (Ren *et al.* 2003). The linker between EF-hands 3 and 4 corresponds to amino acids 14–21 in KChIP2d found to be involved in regulation of Kv4.3 recovery (Patel *et al.* 2002*b*). These data indicate that the N-termini of KChIPs do not significantly contribute to regulatory function, while the C-terminus is essential.

While most KChIPs exert 'conventional' regulatory effects on Kv4 gating (promotion of the slow component of inactivation, acceleration of recovery), a few novel KChIPs have very different properties. KChIP4a has a unique N-terminus containing a 'K^+-channel inactivation suppressor' (KIS) domain which eliminates fast inactivation of Kv4 channels, making them behave as very slowly inactivating delayed rectifiers (Holmqvist *et al.* 2002). KChIP4a is not expressed in heart. However, three cardiac KChIP2 isoforms with either an alternatively spliced C-terminus (KChIP2e, KChIP2f) or N-terminus (KChIP2g) have been identified (Decher *et al.* 2004). KChIP2e *accelerates* Kv4.3 inactivation and *slows* recovery, while KChIP2f slows inactivation but has *no* effect on recovery. In contrast to other KChIP2 isoforms, coexpression of Kv4.3 + KChIP2g generates a hyperpolarizing shift in $V_{1/2}$ of the steady-state inactivation relationship (Decher *et al.* 2004). Functionally, the unique effects produced by these isoforms may further contribute to heterogeneity of I_{to} phenotypes in the LV. Experimentally, these 'unconventional' isoforms could be exploited in coexpression studies to gain new insights into mechanisms governing Kv4 channel gating and KChIP function.

DPPs. Nadal *et al.* (2001) originally demonstrated that coexpression of Kv4.2 with high molecular weight RNA isolated from rat cerebellum resulted in acceleration of inactivation kinetics. The unknown regulatory protein factor was designated 'K^+ Channel *A*ccelerating *F*actor' (KAF). Subsequent studies (Nadal *et al.* 2003) identified KAF as the transmembrane glycoprotein DPP6 (dipeptidyl aminopeptidase related protein 6; Wada *et al.* 1992). Two alternatively spliced isoforms were identified (long, L, and short, S), which differ solely in the length of their cytoplasmic N-termini. Both are integral membrane glycoproteins with a single putative transmembrane domain. The N-terminus is relatively short, while the C-terminus is extensive, consisting of an extracellular matrix binding domain composed of three subdomains: a glycosylation domain, a cysteine-rich domain (possibly

conferring targeting and/or cell adhesion properties to Kv4 channels) and an inactive catalytic domain (Nadal *et al.* 2003).

The regulatory effects of DPP6 on Kv4.2 are very similar to those of KChIP2 isoforms (increased surface expression, acceleration of recovery) except for one fundamental functional difference: DPP6 accelerates Kv4.2 inactivation kinetics, while the majority of KChIP2 isoforms promote the slower component of inactivation. Recently, another dipeptidyl aminopeptidase, DPP10, has also been shown to regulate Kv4.1 and Kv4.2 channels, with effects similar to those produced by DPP6 (Jerng, Qian & Pfaffinger, 2004). This latter work suggests that the intracellular N-terminus of DPP10 is responsible for acceleration of inactivation.

DPP6 and DPP10 are interesting in that they belong to a family of serine proteases but, similar to Kv1-interacting β subunits, lack enzymatic activity (Wada *et al.* 1992). Both appear to be predominantly expressed in brain. If DPPX is found in LV myocytes, then will the DPPX expression gradients across the LV free wall correlate with the functional gradient of $I_{to,fast}$? And how will the effects of DPPXs interact with those of KChIP2 isoforms?

Other potential regulatory subunits. In addition to KChIPs, several other Kv4 regulatory subunits have been studied which have varying effects on Kv4 expression and kinetics. Kvβ1 and β2 increase the expression of Kv4.3 without altering kinetics, while Kvβ1.2 confers redox (O_2) sensitivity to Kv4.2 without altering kinetics (Perez-Garcia *et al.* 1999; Yang *et al.* 2001). KChAP (*K C*hannel *A*ccessory *P*rotein) also increases Kv4.3 expression without effects on kinetics (Wible *et al.* 1998; Kuryshev *et al.* 2000). In contrast, MinK-related peptide 1 (MiRP1) has been reported to alter Kv4.2 gating kinetics (Zhang, Jaing & Tseng, 2001), and the Na^+ channel β_1 subunit interacts 'promiscuously' with Kv4.3, resulting in increased peak current density, accelerated inactivation and slowed recovery (Deschênes & Tomaselli, 2002). Frequenin, another Ca^{2+}-binding protein of the neuronal calcium sensors subfamily, also binds to Kv4 channels and slows inactivation in a Ca^{2+}-dependent manner (Nakamura *et al.* 2001). However, frequenin has no to minimal effects on recovery (Nakamura *et al.* 2001; Guo *et al.* 2002*b*). Any of these subunits could potentially modulate LV I_{to}. At present, the best evidence exists for frequenin, which coimmunoprecipates with Kv4.3 α subunits from mouse heart ventricular extracts (Guo *et al.* 2002*b*; however, see Ren *et al.* 2003). The physiological significance of the other subunits in the heart is still unresolved.

Species differences in LV expression of Kv1.4, Kv4.2, Kv4.3 and KChIP2 isoforms

Compelling evidence indicates that Kv4.2 and/or Kv4.3 underlie generation of LV $I_{to,fast}$. However, there are significant differences among species in both expression profiles and possible role(s) of these two clones in generation of $I_{to,fast}$. The distribution of both K^+ channel and KChIP2 mRNA across the LV free wall has been determined in dog, ferret, human and rat, and measurements of Kv mRNA levels in guinea pig heart have been reported (Dixon & McKinnon, 1994; Dixon *et al.* 1996; Kääb *et al.* 1998; Guo *et al.* 1999; Brahmajothi *et al.* 1999; Rosati *et al.* 2001, 2003; Patel *et al.* 2002*a*,*b*; Nerbonne, 2004; Zicha *et al.* 2004). The mRNA expression patterns obtained from these studies reveal significant heterogeneity across the LV free wall as well as differences between species. With the caveat that mRNA expression does not always imply functional protein expression (Brahmajothi *et al.* 1999; Robertson, 2001), we will summarize the expression data for these six species in relation to the native current distribution(s) observed in LV myocytes isolated from each species.

Human. Kv1.4, Kv4.3 and KChIP2 mRNA are found in the human LV (Kääb *et al.* 1998; Rosati *et al.* 2001). Both KChIP2 mRNA and protein are expressed in a parallel gradient across the LV free wall (LV epi > LV endo), while Kv4.3 mRNA is uniformly expressed within a gradient of Kv4.3 protein (LV epi > LV endo) (Rosati *et al.* 2001; Zicha *et al.* 2004). Based upon these gradients of protein expression, both KChIP2 and Kv4.3 appear to contribute to the $I_{to,fast}$ density gradient across the human LV free wall. Rosati *et al.* (2001, 2003) propose that the KChIP2 mRNA/protein gradient regulates Kv4.3 expression to generate the transmural LV $I_{to,fast}$ gradient. However, expression gradients of KChIP2 and Kv4.3 cannot account for the presence of the cumulatively inactivating $I_{to,slow}$ phenotype in human LV endo myocytes (Näbauer *et al.* 1996; Fig. 2). $I_{to,slow}$ may be mediated by Kv1.4. Kv1.4 mRNA is found in the human LV (Kaab *et al.* 1998), but its distribution has not yet been analysed.

Dog. Kv1.4 mRNA is reported to be present at 16% of the level of Kv4.3 mRNA in the canine LV (Dixon *et al.* 1996). However, there appears to be no electrophysiological evidence for a slowly recovering cumulatively inactivating $I_{to,slow}$ phenotype. Thus, the canine LV free wall appears to express only an $I_{to,fast}$ density gradient. Consistent with this functional observation, the canine LV free wall displays gradients of both KChIP2 and Kv4.3 protein (LV epi > LV endo) that closely parallel the LV transmural $I_{to,fast}$ gradient (Rosati *et al.* 2001, 2003; Zicha *et al.* 2004).

A recent controversy has arisen over the physiological significance of KChIPs in regulation of LV $I_{to,fast}$. While the majority of investigators agree on the importance of KChIP2 isoforms in regulation of $I_{to,fast}$, using a polyclonal KChIP2 antibody Deschênes *et al.* (2002) failed

to detect an expression gradient across the canine LV free wall. As suggested by both Rosati *et al.* (2003) and Zicha *et al.* (2004), a plausible explanation is that the antibody employed by Deschênes *et al.* (2002) possessed insufficient selectivity for KChIP2 protein, resulting in non-specific binding that obscured the gradient. We agree with this explanation.

Ferret. Similar to human, ferret LV free wall exhibits both density and phenotypic gradients of $I_{to,fast}$ and $I_{to,slow}$. Kv4.2 protein is mainly localized to LV epi while Kv4.3 protein is transmurally expressed across the LV free wall. However, while Kv1.4 mRNA is expressed uniformly across LV free wall Kv1.4 protein is localized almost exclusively to the LV endo (Brahmajothi *et al.* 1999; Fig. 9*A*).

These results raise the question: given the presence of Kv1.4 and Kv4.3 protein why is $I_{to,fast}$, or a mixed $I_{to,fast}/I_{to,slow}$ phenotype, not observed in the majority of ferret LV endo myocytes (Brahmajothi *et al.* 1999)? An answer likely resides in the fact that, similar to human and dog, there is an expression gradient of KChIP2 (mRNA and protein) across the ferret LV free wall (LV epi > LV endo; Patel *et al.* 2002*a*,*b*). These results are consistent with the proposal of Rosati *et al.* (2001) that reduced KChIP2 expression may minimize functional Kv4.3 expression.

The ferret LV free wall also displays a gradient of Kv4.2 protein (LV epi > LV endo) that parallels the $I_{to,fast}$ gradient (Brahmajothi *et al.* 1999). It is thus unclear if LV epi $I_{to,fast}$ is due to Kv4.2, Kv4.3 and/or Kv4.2/Kv4.3 heteromultimers (Nerbonne, 2002). Nonetheless, the distributions of Kv1.4, Kv4.2, Kv4.3 and KChIP2b proteins argue for both I_{to} density and phenotypic gradients. However, the mechanisms regulating Kv1.4 protein expression in ferret LV endo but not LV epi myocytes in the presence of uniform mRNA expression levels are unknown. Could such mechanisms also be responsible for the lack of $I_{to,slow}$ in dog LV even though Kv1.4 mRNA can be measured (Dixon *et al.* 1996)?

Rat. Electrophysiological studies indicate the presence of both I_{to} density and phenotypic gradients across the rat LV free wall (Clark *et al.* 1993; Casis *et al.* 1998). Analyses of Kv4.2 and Kv4.3 mRNA reveal distributions similar to those in ferret LV, with uniform expression of Kv4.3 amid a transmural gradient of Kv4.2 (LV epi > LV endo; Dixon & McKinnon, 1994; Dixon *et al.* 1996; Rosati *et al.* 2001). However, expression of KChIP2 mRNA is uniform (Rosati *et al.* 2001). Rosati *et al.* (2001) thus concluded that the Kv4.2 gradient is responsible for the $I_{to,fast}$ density gradient. While plausible, this hypothesis raises the question: why does the uniform distribution of Kv4.3 and KChIP2 mRNA not result in uniform $I_{to,fast}$ expression? Are there mechanisms preventing Kv4.3 and/or KChIP2 protein expression in rat LV endo myocytes?

Kv1.4 mRNA is also expressed uniformly across the rat LV. If Kv1.4 protein expression in the rat LV is similar to that of the ferret (where Kv1.4 mRNA expression is uniform but Kv1.4 protein localizes to the LV endo; Brahmajothi *et al.* 1999), then Kv1.4 could account for localization of $I_{to,slow}$.

Mouse. Initial studies indicated heterogeneous expression of $I_{to,fast}$ and $I_{to,slow}$ in mouse heart, with $I_{to,fast}$ being expressed in the LV apex and $I_{to,slow}$ in the interventricular septum (Xu *et al.* 1999). Another extensive analysis of I_{to} phenotype expression in the mouse heart has recently been conducted by Brunet *et al.* (2004). While $I_{to,fast}$ was observed in all LV myocyte types (apex, base, epi, endo), peak current density was higher in apical and LV epi myocytes than in either basal or LV endo myocytes. No evidence could be found for $I_{to,slow}$ expression in any LV free wall myocyte type. Thus, in mouse it appears that: (i) $I_{to,slow}$ is present only in the interventricular septum; and (ii) in the LV there are significant apical-to-basal and epicardial-to-endocardial expression gradients of $I_{to,fast}$ (similar to that predicted for ferret LV; Brahmajothi *et al.* 1999; Fig. 9*A*). At the molecular level, there appears to be a general consensus that the $I_{to,fast}$ gradient across the normal murine LV free wall is due to heterogeneous expression of Kv4.2 (LV epi > LV endo) amid a background of uniform KChIP2 expression (e.g. Guo *et al.* 1999; Rosati *et al.* 2003; Brunet *et al.* 2004).

Transgenic mouse techniques have further helped dissect the molecular components underlying murine I_{to} phenotypes (London, 2001; Nerbonne, 2004). Targeted deletion of the Kv1.4 gene, *Kv1.4*$^{-/-}$, eliminates $I_{to,slow}$ in mouse septal myocytes but has no effect on $I_{to,fast}$ in LV myocytes (London *et al.* 1998*b*). LV $I_{to,fast}$ can be completely eliminated by either targeted deletion of the Kv4.2 gene (*Kv4.2*$^{-/-}$; Guo *et al.* 2000) or expression of the dominant negative (DN) pore mutant Kv4.2W362F (Barry *et al.* 1998). Mice expressing a dominant-negative truncated Kv4.2 (*Kv4.2N*) display significantly reduced (but not completely eliminated) $I_{to,fast}$ (Wickenden *et al.* 1999). Finally, $I_{to,fast}$ is eliminated in mice with a targeted deletion of the KChIP2 gene, *KChIP2*$^{-/-}$ (Kuo *et al.* 2001).

All four of these genetic manipulations (*Kv4.2DN*, *Kv4/2*$^{-/-}$, *Kv4.2N*, *KChIP2*$^{-/-}$) result in prolonged LV myocyte action potentials. However, although there is a complete loss of $I_{to,fast}$ in *Kv4.2 DN* and *Kv4.2*$^{-/-}$ mice, these mice do not display increased susceptibility to arrhythmias (Barry *et al.* 1998; Guo *et al.* 2000; Brunner *et al.* 2001). In contrast, *Kv4.2N* mice display several serious pathologies, including cardiac hypertrophy, fibrosis and sudden death (Wickenden *et al.* 1999). *KChIP2*$^{-/-}$ mice also display increased susceptibility to ventricular tachycardia and sudden death (Kuo *et al.* 2001). Thus, functional conclusions on the role of $I_{to,fast}$ in generation of LV pathologies, as well as its contribution to the ECG,

appear to be highly dependent upon the particular mouse model. Reasons underlying these functional discrepancies have yet to be clarified. A further discussion of potential limitations associated with transgenic approaches can be found in Nerbonne (2004).

Guinea pig. No measurable I_{to} phenotype ($I_{to,fast}$ or $I_{to,slow}$) exists in guinea pig LV myocytes. Consistent with this observation Kv1.4, Kv4.2 and Kv4.3 mRNA are all undetectable in guinea pig heart (Zicha *et al.* 2003).

Conclusion. To conclude this section, it should be noted that use of the relative terms 'fast' *versus* 'slow' is not always consistent among different laboratories. We thus feel it is important to emphasize that in the absence of KChIP2 isoforms, Kv4.2/4.3 recovery time constants are still approximately an order of magnitude *faster* than those of Kv1.4/$I_{to,slow}$, and neither Kv4.2 nor Kv4.3 displays cumulative inactivation, in either the absence or the presence of KChIP2 isoforms. We propose that 'fast' be used to denote recovery kinetics with time constants on the order of *tens* of milliseconds (Kv4.2/4.3 + KChIP2 isoforms), 'intermediate' recovery kinetics with time constants on the order of *hundreds* of milliseconds (Kv4.2/4.3 with reduced to no KChIP expression) and 'slow' recovery kinetics with time constants on the order of *thousands* of milliseconds (Kv1.4). If such a nomenclature is valid, then, in contrast to $I_{to,slow}$, both $I_{to,fast}$ and $I_{to,intermediate}$ would display HPTX/PaTX sensitivity, closed-state reverse use-dependent block by 4-AP and little to no cumulative inactivation. Of course, this nomenclature is based upon the predicted effects of KChIP2 isoform gradients. If additional regulatory subunits are expressed in LV myocytes it is unclear how they may alter this scenario.

I_{to} phenotype expression in Purkinje fibres

While the first cardiac I_{to} phenotype appears to have been recorded in sheep Purkinje fibres (Deck & Trautwein, 1964), very limited data exist at present on the molecular and biophysical bases of Purkinje fibre I_{to} phenotypes. Recent studies have been conducted on single Purkinje fibres isolated from free-running endocardial false tendons of canine and human hearts (Han *et al.* 2000, 2002*a*,*b*). In both species, an I_{to} can be recorded that displays: (i) biexponential inactivation kinetics (fast time constants on the order of milliseconds, slow time constants on the order of tens of milliseconds); (ii) biexponential recovery kinetics (fast time constants on the order of tens of milliseconds, slow time constants on the order of thousands of milliseconds); and (iii) prominent cumulative inactivation. These observations suggest a mixture of $I_{to,fast}$ and $I_{to,slow}$ phenotypes; however, the Purkinje fibre I_{to} phenotype displays significant differences from both Kv4.2/4.3-mediated $I_{to,fast}$ and Kv1.4-mediated $I_{to,slow}$ in its sensitivity to 4-AP, tetraethylammonium$^+$ and cellular redox state.

At the molecular level (both mRNA and protein), Han *et al.* (2002*a*) report that canine Purkinje fibres express extremely low levels of Kv1.4, no detectable levels of Kv4.2, and levels of Kv4.3 comparable to LV midmyocardial myocytes. KChIP2 mRNA was also found to be much less abundant in Purkinje fibres than LV midmyocardial myocytes. Interestingly, Kv3.4 mRNA and protein were reported to be abundantly expressed (see also Brahmajothi *et al.* 1996). Kv3.4 channels generate a TEA$^+$-sensitive I_{to} phenotype (e.g. Vega-Saenz de Miera *et al.* 1992).

The results of Han *et al.* (2000, 2002*a*,*b*) would indicate that the Purkinje fibre I_{to} phenotype is unique and predominantly due to Kv3.4 subunits. However, Purkinje fibres possess a hyperpolarization-activated cation current ('I_f'; Campbell *et al.* 1992). It is unclear if deactivating I_f currents may be contributing to the reported Purkinje fibre I_{to} characteristics (Verkerk & van Ginneken, 2001; Boyett *et al.* 2001). This is an important issue that needs to be addressed in future Purkinje fibre studies.

Molecular and biophysical mechanisms of activation, inactivation and recovery

Kv1.4. Activation of Kv1.4 is sigmoidal and can be described using a Hodgkin-Huxley-like 'a^4' formulation (Hodgkin & Huxley, 1952; Comer *et al.* 1994), implying the presence of multiple closed channel states. With regard to inactivation, classic studies on Shaker channels demonstrated the presence of two inactivation mechanisms, N-type (N-terminal 'ball-and-chain' mechanism) and C-type (pore closure mechanism) (Hoshi *et al.* 1990, 1991; Zagotta *et al.* 1990; Choi *et al.* 1991; Wissmann *et al.* 2003). Both of these mechanisms are present in cardiac Kv1.4 channels. Mutagenesis studies support the hypothesis that these two mechanisms are allosterically coupled, with N-type inactivation controlling the rapid component of inactivation and C-type inactivation controlling cumulative inactivation and the very slow kinetics of recovery (Rasmusson *et al.* 1995*a*; Roeper *et al.* 1997). The detailed molecular and biophysical characteristics of Shaker N- and C-type inactivation mechanisms have been extensively reviewed (Rasmusson *et al.* 1998; Yellen, 1998, 2002; Wissmann *et al.* 2003). We direct readers to the following sources for detailed discussion of N-type and C-type inactivation mechanisms and their relevance to cardiac Kv1.4/$I_{to,slow}$ gating mechanisms: Rasmusson *et al.* (1995*a*,*b*, 1998), Roeper *et al.* (1997), Oudit *et al.* (2001), Jiang *et al.* (2003*a*), Li *et al.* (2003) and Bett & Rasmusson (2004).

Kv4.2/4.3. The molecular mechanisms underlying the biophysical gating characteristics of Kv4.2/4.3 are not

as clearly delineated as Kv1.4. Nevertheless, significant progress has occurred in this area over the past several years.

Activation. Two recent independent studies have demonstrated that activation of Kv4.3 channels is sigmoidal and can be well-described using a Hodgkin-Huxley-like 'a^4' formulation (Hodgkin & Huxley, 1952; Patel *et al.* 2004; Wang *et al.* 2004). $\tau_{activation}$ values display saturation at depolarized potentials, indicating a voltage-independent rate-limiting step(s). Also, since inactivation of Kv4.3 is approximately an order of magnitude slower than activation, fits to the early phases of activation are not seriously distorted by inactivation. To account for saturation of rate constants, Patel *et al.* (2004) empirically fitted their observed $\tau_{activation}-V_m$ curves with Boltzmann-like functions, while Wang *et al.* (2004) proposed the following discrete state Markov model consisting of five closed states and one open state, with voltage-dependent rate constants (α and β) for transitions between with the first four closed states and voltage-independent rate constants (k_{co} and k_{oc}) for transition between the final preactivated closed-state and open-state:

$$\mathrm{CO} \underset{\beta}{\overset{4\alpha}{\rightleftharpoons}} \mathrm{C1} \underset{2\beta}{\overset{3\alpha}{\rightleftharpoons}} \mathrm{C2} \underset{3\beta}{\overset{2\alpha}{\rightleftharpoons}} \mathrm{C3} \underset{4\beta}{\overset{\alpha}{\rightleftharpoons}} \mathrm{C4} \underset{k_{oc}}{\overset{k_{co}}{\rightleftharpoons}} \mathrm{O} \qquad \text{Scheme 1}$$

Two interesting additional observations were that: (i) Increasing $[K^+]_o$ (2–98 mM) stabilized the channel open state, as manifested by a slowing in the kinetics of deactivation; and (ii) the voltage dependence of $\tau_{activation}$ was best described as a biexponential process, suggesting two different populations of gating charges (Wang *et al.* 2004). These two charges (in 2 mM $[K^+]_o$) are estimated to be $0.27e_o$ and $2.11e_o$ per subunit. At very depolarized or hyperpolarized potentials movement of the larger charge component is hypothesized to become essentially instantaneous, while movement of the smaller component becomes dominant and rate limiting. Activation of Kv4 channels may thus be more complex than Shaker channels.

The steepness of the steady-state activation curve for Kv4 channels is typically 2–3 times less than that observed for Shaker channels, with slope factor values for a single subunit of ~19–25 mV (e.g. Bähring *et al.* 2001*a*; Beck *et al.* 2002; Wang *et al.* 2004). As pointed out by Wang *et al.* (2004) this observation may have one physical basis in significant differences between the amino acid sequences of S4 in Shaker *versus* Kv4 channels: (i) Shaker has seven positive charges, while Kv4.3 has only five; and (ii) there are seven differences among uncharged residues.

Shaker S4	I	L	R	V	I	R	L	V	R	V	F	R	I	F	K	L	S	R	H	S	K	G	L
Kv4.3 S4	A	F	V	T	L	R	V	F	R	V	F	R	I	F	K	F	S	R	H	S	Q	G	L
			+		+		+		+		+		+										

Inactivation and recovery. In contrast to Kv1.4, the molecular basis of inactivation and recovery of Kv4 channels is unclear. All Kv4 channels inactivate as multiexponential processes, suggesting multiple mechanisms (Bähring *et al.* 2001*a*; Beck *et al.* 2002; Patel *et al.* 2002*a*,*b*; Shahidulla & Covarrubias, 2003; Hatano *et al.* 2004). However, the fractional contributions of the different components of inactivation vary considerably among family members. For example, under 'basal' conditions Kv4.1 inactivation occurs predominantly through the slow component, while Kv4.3 inactivation is dominated by the fast component (Jerng & Corvarrubias, 1997; Jerng *et al.* 1999; Beck & Corvarrubias, 2001; Patel *et al.* 2002*a*,*b*, 2004). Further appraisal of the literature suggests that multiple channel domains may be involved in these processes, but also reveals conflicting conclusions and debate on underlying molecular mechanisms.

Due to the predominance of early studies on Shaker channels, which demonstrated allosteric coupling between N- and C-type inactivation (Hoshi *et al.* 1990, 1991; Choi *et al.* 1991; Rasmusson *et al.* 1998; Yellen, 1998, 2002), initial studies focused on the potential involvement of these two mechanisms in regulating Kv4 channel inactivation and recovery. In contrast to the criteria established for characterization of 'classic' N- and C-type mechanisms, these studies demonstrated that: (i) neither extracellular nor intracellular tetraethylammonium altered inactivation (Jerng & Corvarrubias, 1997); (ii) increasing $[K^+]_o$ *accelerated* inactivation and *slowed* recovery (Jerng *et al.* 1999); and (iii) N-terminal deletion did not slow the kinetics of closed-state inactivation or alter the kinetics of recovery (Bähring *et al.* 2001*a*). It was thus concluded that Kv4 channels lacked N- and C-type mechanisms as originally defined for Shaker channels, although it was proposed that concerted interactions of unspecified regions of the cytosolic N- and C-termini and regions near the internal mouth of the pore were involved in regulating inactivation (Jerng *et al.* 1999). However, it has recently been suggested (Gebauer *et al.* 2004) that the N-terminus of Kv4.2 can act as an N-type inactivation peptide under certain heterologous coexpression conditions. This has been confirmed by Pourrier *et al.* (2004), who demonstrated that attachment of the Kv4.2 N-terminus to N-terminus-deleted Kv1.4 both restored rapid inactivation and accelerated recovery. The latter result suggests that the Kv4.2 N-terminus may act as an inactivation ball. However, it is less efficient in promoting Kv1.4 N-type inactivation than the native Kv1.4 N-terminus inactivation ball(s) (Rasmusson *et al.* 1995*a*; Wissmann *et al.* 2003). While these results are of high intrinsic molecular and biophysical interest, their physiological significance to LV I_{to} is unclear.

Additional studies have yielded intriguing results on regions (other than the N-terminus) of Kv4 channels that may also be involved in regulation of inactivation and recovery. The following three observations are of particular interest.

(i) Mutation of a cysteine to a serine in the S4–S5 loop of Kv4.1 (C322S) slowed both inactivation and deactivation (Jerng *et al.* 1999) with little effect on recovery.

(ii) Amino acids 420–429 in the Kv4.3 C-terminus have been demonstrated to regulate the voltage dependence of recovery (Hatano *et al.* 2004). When two arginines in this region were both mutated to alanines (R426A, R429A) there was no effect on inactivation but a dramatic slowing of recovery. We are unaware of any other Kv4.3 mutation that has such unique effects on recovery but not inactivation.

(iii) A mutation near the inner mouth of the Kv4.1 pore (V(404,406)I) dramatically slows inactivation (Jerng *et al.* 1999), while a similar mutation in Kv4.3 (V(399,401)I) results in only modest effects on inactivation (Wang *et al.* 2002). These results suggest that this mutation targets the slow component of inactivation that is more dominant in Kv4.1 than Kv4.3, and emphasize the important kinetic differences between members of the Kv4 family. Furthermore, since most KChIPs produce gating shifts promoting the slower component of inactivation, it is interesting to note that coexpression of KChIP2b with the Kv4.3(V(399,401)I) pore mutant results in a dramatic slowing of inactivation (Wang *et al.* 2002), an effect very similar to that produced by the Kv4.1 (V(404,406)I) pore mutant expressed alone (Jerng *et al.* 1999). Is this indicating that KChIP-mediated promotion of the slower component of Kv4.3 inactivation involves allosteric interactions with the inner vestibule of the channel pore?

While these three sets of results remain to be mechanistically explained, they suggest that regions of the C-termini and inner pore vestibule are involved in regulation of Kv4 channel inactivation and recovery. Different regions of the channel complex may also control inactivation and recovery separately. No proposed Kv4 channel or native phenotypic I_{to} gating model can account for all of these observations (Campbell *et al.* 1993*a*,*b*; Greenstein *et al.* 2000; Winslow *et al.* 2000; Puglisi & Bers, 2001; Bähring *et al.* 2001*a*; Rudy, 2002; Beck *et al.* 2002; Bondarenko *et al.* 2004; Jerng, Qian & Pfaffinger, 2004; Wang, Puglisi & Bers, 2004; Iyer *et al.* 2004; Winslow *et al.* 2005).

Speculation: voltage dependence of $I_{to,fast}$ recovery kinetics. Kv4.2/4.3 inactivation kinetics are voltage independent at only moderately depolarized potentials, while recovery kinetics are voltage dependent over the entire physiological range of hyperpolarized potentials (e.g. Campbell *et al.* 1993*b*; Patel *et al.* 2004). How can inactivation be voltage independent but recovery voltage dependent? And how can intracellular KChIPs accelerate recovery in a voltage-dependent manner?

Three independent sets of data may be hinting at mechanisms: (i) Kv4.3 activation and inactivation are likely to be coupled (Patel *et al.* 2004; Wang *et al.* 2004); (ii) increases in $[K^+]_o$ slow both Kv4 recovery (Jerng *et al.* 1999) and deactivation (Wang *et al.* 2004); and (iii) KChIPs accelerate Kv4.3 recovery and deactivation (Patel *et al.* 2002*a*,*b*, 2004). These results may indicate that channel regions regulating recovery and deactivation are coupled. Could 'reverse' movement of S4 impart voltage dependence to recovery, a mechanism similar to that originally proposed for the voltage-gated sodium channel (Patlak, 1991)? Does the fact that recovery and deactivation are both $[K^+]_o$ and KChIP dependent indicate allosteric coupling between the gondola, pore domain(s) and movement of S4? And could provision of KChIP-mediated allosteric coupling be the primary role of the N- and/or C-termini of Kv4 channels?

Unique properties and mechanisms of regulation of distinct LV I_{to} phenotypes

$I_{to,fast}$ *versus* $I_{to,slow}$: regulation of frequency-dependent action potential characteristics. Action potential (AP) recordings from rabbit, rat and ferret LV myocytes demonstrate significant differences in frequency-dependent modulation of AP morphologies. In canine LV epi and LV endo myocytes, increasing stimulation frequency leads to a shortening of AP duration, which is consistent with the transmural gradient of $I_{to,fast}$ (Fig. 11*A*). In rabbit, where $I_{to,slow}$ is expressed in all LV myocyte types, increasing pulse frequency leads to an *increase* in AP duration (Fig. 11*B*). In both rat and ferret LV epi myocytes, increasing pulse duration leads to a decease in AP duration; in contrast, in LV endo myocytes increasing pulse frequency leads to an increase in AP duration (Fig. 11*C* and *D*). Thus, in some species the combination of $I_{to,fast}$ and $I_{to,slow}$ contributes to the generation of *opposite* frequency-dependent effects on APs in LV epi *versus* LV endo myocytes: during periods of increased stimulation, the predominance of $I_{to,fast}$ correlates with decreased AP durations while the predominance of $I_{to,slow}$ correlates with increased AP durations. While AP morphology is the summed result of *all* currents flowing across the sarcolemma, these results are consistent with the predicted effects of the distinct inactivation and recovery kinetics of Kv4.2/4.3-mediated *versus* Kv1.4-mediated I_{to} phenotypes.

Many investigators have hypothesized that differences in action potential morphologies between distinct LV myocyte types would produce significant repolarization gradients across the LV free wall, and that such gradients may be the source of the T-wave of the electrocardiogram (Gussack & Antzelevitch, 2003). However, numerous whole LV tissue and *in vivo* animal heart studies have consistently failed to demonstrate the predicted transmural repolarization gradients (Taggart *et al.* 2003). It is unclear whether this discrepancy is due to technical difficulties (use of bipolar electrodes in whole tissue;

absence of electrotonic coupling in isolated myocytes). However, in species possessing an LV epi $I_{to,fast}$–LV endo $I_{to,slow}$ phenotypic gradient (e.g. ferrets, humans), the *opposite* frequency-dependent regulatory effects that these two I_{to} phenotypes exert on LV epi and LV endo myocyte action potentials would contribute to *minimizing* transmural repolarization gradients at normal heart rates. Thus, in such species the LV epi $I_{to,fast}$–LV endo $I_{to,slow}$ gradient would be inherently antiarrhythmic under normal conditions. If correct, then in such species the normal T-wave would arise from other more global repolarization gradients (apical–basal, RV–LV; de Bakker & Opthof, 2002; Taggart *et al.* 2003). Under pathological conditions, alterations in $I_{to,fast}$ and/or $I_{to,slow}$ could lead to alterations in conduction and/or generation of transmural LV repolarization gradients contributing to abnormal T-wave activity (Huelsing *et al.* 2003; Libbus *et al.* 2004). These considerations also argue for caution when applying LV myocyte computer models that only incorporate differences in peak density of a single I_{to} phenotype to results obtained from whole LV tissue (Winslow *et al.* 2005).

Speculation: regulation of $I_{to,slow}$ and $I_{to,fast}$ by phosphorylation. $I_{to,slow}$. The AP results obtained from rabbit LV and rat and ferret LV endo myocytes (Fig. 11) strongly argue that $I_{to,slow}$ can be an important repolarizing current at low heart rates. However, due to its very slow recovery kinetics and cumulative inactivation it is assumed by many investigators that Kv1.4 plays no significant role in repolarization at normal heart rates. This may be correct; however, a study on the effects of Ca^{2+}/calmodulin-dependent protein kinase II (CaMKII) on Kv1.4 kinetics raises a significant challenge to this assumption (Roeper *et al.* 1997). Roeper *et al.* (1997) demonstrated that CaMKII is capable of phosphorylating

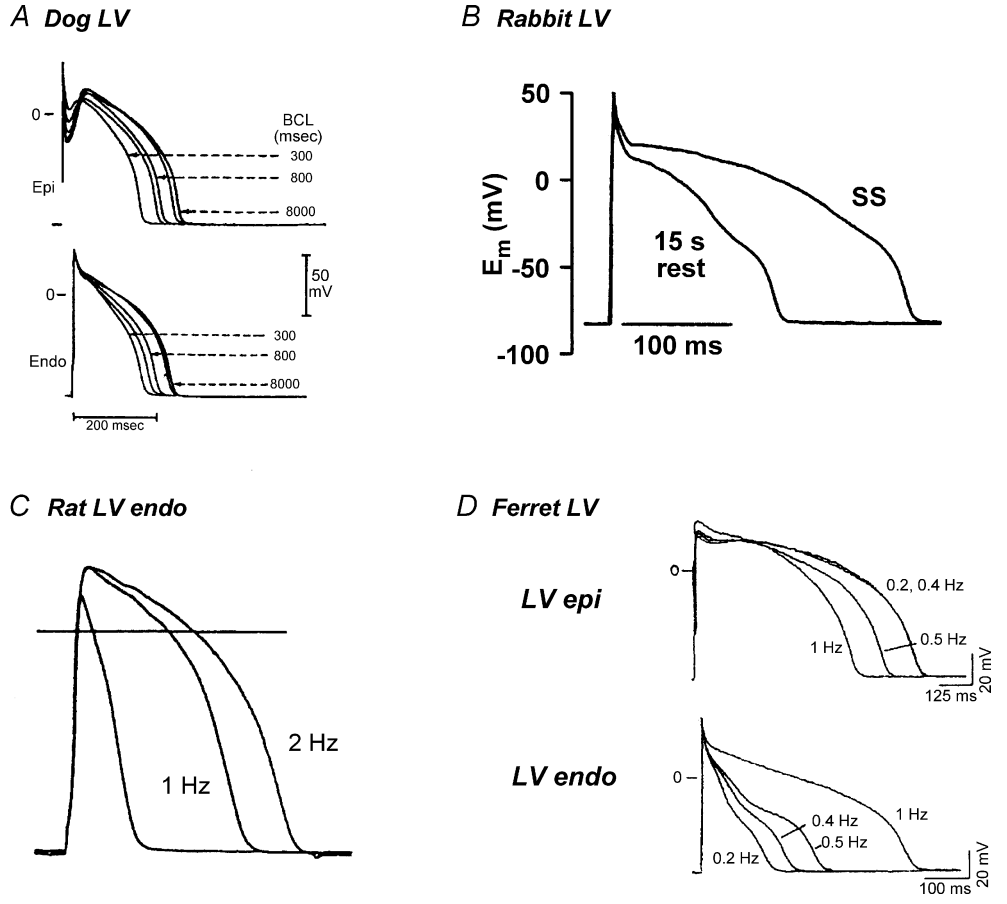

Figure 11. Frequency-dependent characteristics of action potential (AP) morphologies in LV myocytes of different species: predominance of effects of $I_{to,fast}$ *versus* $I_{to,slow}$
A, APs of dog LV epi and LV endo myocytes elicited at increasing basic cycle lengths (BCL) of stimulation from 8000 ms to 300 ms. *B*, rabbit LV myocyte after 15 s of rest and final 20th steady-state (SS) AP elicited at 0.5 Hz. *C*, rat LV endo myocyte APs at rest, 1 Hz and 2 Hz. *D*, APs of ferret LV epi and LV endo myocytes with stimulation frequency progressively increased from 0.2 to 1 Hz. Final 20th steady-state AP at end of each pulse train is illustrated. Data from: dog, Liu *et al.* (1993) with permission of Lippincott Williams & Wilkins; rabbit, Bassani *et al.* (2004); rat, Shimoni *et al.* (1995); ferret, D. L. Campbell, unpublished results, recording conditions as described in Campbell *et al.* (1993*b*).

Kv1.4 α subunits at serine residue 123. More intriguing were the observations that phosphorylation resulted in marked slowing of inactivation kinetics, pronounced reduction of cumulative inactivation and a 10-fold acceleration of recovery kinetics, with time constants on the order of *hundreds* of milliseconds (Fig. 12). These CaMKII-mediated effects were dependent upon $[Ca^{2+}]_i$.

Roeper *et al.* (1997) propose that phosphorylation of Kv1.4 results in acceleration of recovery from N-type inactivated states, while dephosphorylation results in increased 'trapping' in C-type inactivated states, with the latter resulting in cumulative inactivation and slowed recovery (Rasmusson *et al.* 1995*a*). If correct, then the slow recovery and cumulative inactivation of Kv1.4 under 'basal' conditions (Fig. 6) would be due to dephosphorylated channels and predominance of C-type inactivation. Similarly, due to the presence of Ca^{2+} chelators in whole cell patch pipettes, slow recovery and cumulative inactivation of LV $I_{to,slow}$ (Fig. 2) would be due to reduced CaMKII activity and dephosphorylated Kv1.4 channels. These results raise an interesting question for cardiac cellular electrophysiologists: under normal conditions of cyclically changing $[Ca^{2+}]_i$ within LV endo myocytes does $I_{to,slow}$ inactivation decrease and recovery accelerate? And, if so, how does this relate to the regulation of frequency-dependent modulation of action potential morphologies in LV endo myocytes (Fig. 11)?

$I_{to,fast}$: obligatory involvement of KChIP2 isoforms in kinase-mediated modulatory effects? Adenylate cylcase, protein kinase A (PKA) and protein kinase C (PKC) isoforms are all potential physiological regulators of native LV $I_{to,fast}$. For example, in many species, the distribution of $I_{to,fast}$ correlates with positive inotropic effects produced by α_1-adrenergic receptor stimulation (Fedida *et al.* 1993). Voltage clamp studies indicate that α_1-receptor stimulation inhibits LV $I_{to,fast}$ and that these effects may be due to activation of PKC (Parker & Fedida, 2001). With regard to PKA, Schrader *et al.* (2002) demonstrated that PKA-mediated phosphorylation of Kv4.2 expressed alone generated no regulatory effects. However, PKA-mediated effects were 'rescued' when Kv4.2 was coexpressed with KChIP3. Regulatory effects of phosphorylation in the presence of KChIP3 included a reduction in peak current amplitude and slowing of inactivation, but no additional effects on recovery. Between the two potential phospholylation sites, Thr 38 and Ser 552 (Anderson *et al.* 2000), only Ser 552 was found to be essential (Schrader *et al.* 2002). KChIP3 association is thus an obligatory prerequisite for PKA-mediated phosphorylation of Kv4.2. If similar effects are displayed by LV $I_{to,fast}$, then KChIP2

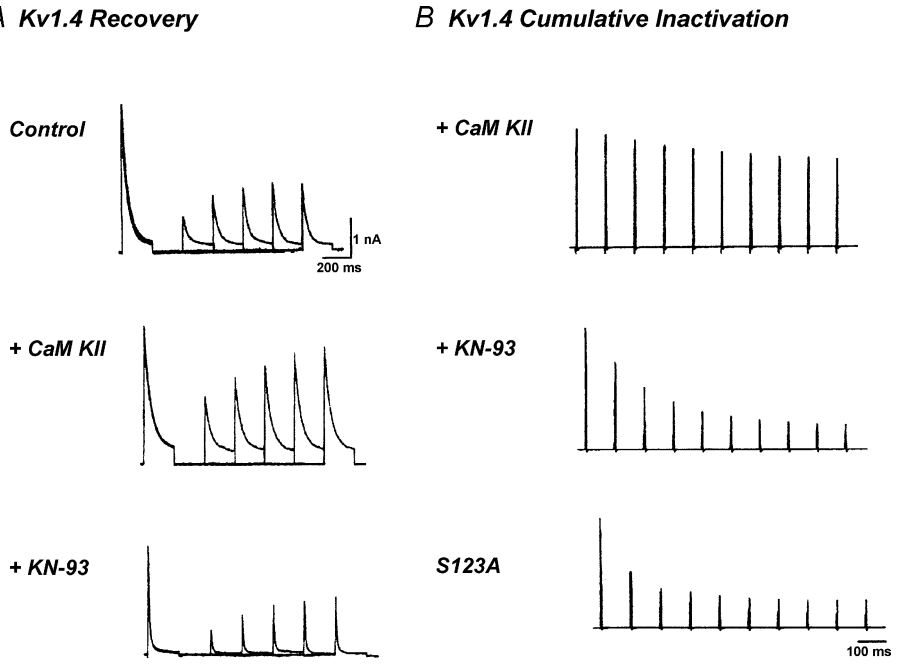

Figure 12. Regulation of Kv1.4 inactivation and recovery kinetics by CaMKII-mediated phosphorylation (HEK-293 cells, perforated patch technique)
A, recovery waveforms (HP = −80 mV) for Kv1.4 alone (control), after microinjection with autothiophosphorylated CaMKII (+ CaM KII) and after 30 min preincubation in 10 μM KN-93 (CaMKII blocker). *B*, cumulative inactivation waveforms in the presence of CamKII, after KN −93 preincubation, and in the presence of the Kv1.4 S123A mutation. Currents were repetitively stimulated at 10 Hz (5 ms depolarizations to +20 mV from HP = −60 mV). Both KN-93 and the S123A mutation prevented CaMKII-mediated reduction of Kv1.4 cumulative inactivation. Data from Roeper *et al.* (1997); © 1997 by the Society for Neuroscience.

isoforms may be critical determinants for PKA-dependent modulation of distinct LV I_{to} phenotypes: regulation of $I_{to,fast}$ would have an obligatory dependence upon KChIP2 isoforms. This prediction awaits experimental verification.

Speculation: $[Ca^{2+}]_i$, KChIP2 isoforms and $I_{to,fast}$. Kinetic analysis of $I_{to,fast}$ in LV myocytes requires block of $I_{Ca,L}$ and highly buffered $[Ca^{2+}]_i$ solutions, manoeuvres which eliminate the $[Ca^{2+}]_i$ transient. Thus, under conventional whole cell patch clamp conditions Kv4.2/4.3-mediated I_{to} recovery would still be accelerated by KChIP2 isoforms but the slow component of inactivation would be minimized (Patel *et al.* 2002*b*, 2004). However, in an intact LV epi myocyte under physiological conditions the situation may be very different: due to the overlap of $I_{to,fast}$, $I_{Ca,L}$ and the $[Ca^{2+}]_i$ transient, the Ca^{2+}-bound KChIP-dependent slow component of inactivation would be promoted, thus making $I_{to,fast}$ a much more prominent hyperpolarizing current during *all* phases of the action potential plateau. In addition, if the predictions of the model of Patel *et al.* (2004) are correct, then Ca^{2+}-bound KChIP-promoted reopening of Kv4.2/4.3 channels would contribute to final phase 3 repolarization. Thus the conventionally predicted behaviour of $I_{to,fast}$ during an LV myocyte action potential (Fig. 1) may not be correct. These predictions are speculative, and the physiological importance of such 'cross-talk' interactions between $I_{to,fast}$, $I_{Ca,L}$ and the $[Ca^{2+}]_i$ transient have yet to be demonstrated. But if these predictions are verified, then KChIP2 isoforms would be prime candidates for the development of selective antiarrhythmic agents (Strauss & Rasmusson, 2002; Sanguinetti & Bennet, 2003).

Biophysical gating models and recent molecular insights

Proposed gating models

Kv1.4/$I_{to,slow}$. The classic analysis by Aldrich (1981) on the cumulatively inactivating I_A in *Archidoris* and *Anisodoris* neurones provided the original gating model for what is now recognized as the LV $I_{to,slow}$ phenotype. This model consisted of four channel states:

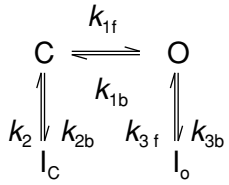

Scheme 2

Upon depolarization, channels either rapidly inactivate (I) from the resting state (C) or more slowly inactivate from the open state (O). This model was subsequently applied to rabbit atrial myocyte $I_{to,slow}$ (Clark *et al.* 1988). During rapid and repetitive voltage clamp pulses, cumulative inactivation results from rapid closed-state inactivation and slower recovery from the open inactivated state, a process now known to be controlled by C-type inactivation (Rasmusson *et al.* 1995*a*; Roeper *et al.* 1997). Although such simple four-state models cannot account for sigmoid activation kinetics, they do successfully reproduce the basic inactivation and recovery properties of $I_{to,slow}$. These models also predict reopening currents upon membrane hyperpolarization (Ruppersberg *et al.* 1991*a*; Demo & Yellen, 1991; Patel *et al.* 2004). However, at the molecular level these models cannot account for coupling between N-type and C-type inactivation. Thus, a 'more realistic' model of Kv1.4 gating might be:

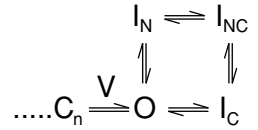

Scheme 3

where C_n is the final closed state, V denotes the final voltage-sensitive transition, I_N is the N-type inactivated state, I_C the C-type inactivated state and I_{NC} the simultaneously N- and C-type inactivated state (Hoshi *et al.* 1990, 1991; Rasmusson *et al.* 1995*a*, 1998; Yellen, 2002). If the model of Roeper *et al.* (1997) is applicable, CaMKII-mediated phosphorylation would increase recovery by promoting the I_N state.

Kv4.2/4.3/$I_{to,fast}$. There are currently several Kv4 gating models. In general, these models agree on the predominance of closed-state inactivation in Kv4 gating; however, they differ on the assignment of kinetic transitions to specific channel conformational states (closed, open, inactivated), number of exponential components of macroscopic inactivation (2 *versus* 3), regulatory effects of varying $[K^+]_o$ and KChIPs on gating and presence/predominance of reopening currents upon membrane hyperpolarization (Ruppersberg *et al.* 1991*a*; Demo & Yellen, 1991; Bähring *et al.* 2001*a*; Beck *et al.* 2002 Patel *et al.* 2004).

Kv4 'allosteric' models. These models are based upon triple exponential descriptions of Kv4 channel inactivation kinetics (Bähring *et al.* 2001*a*; Beck *et al.* 2002). Their central proposal is that upon entering the open state (O) Kv4 channels may transiently enter a non-absorbing open-inactivated state (I_O) but ultimately accumulate in a closed-inactivated state (I_C). It is from the I_C state that channels directly recover. Thus, recovery would be an 'electrically silent' process due to the absence of reopening currents. In these models an 'allosteric factor (f)' is introduced to favour inactivation from preactivated closed-states 'nearer' to the open state.

Bähring *et al.* (2001*a*) proposed an allosteric model as a descriptor of Kv4.2 channel gating. This model was based upon the observations that Kv4.2 N-terminal deletion

did not affect recovery from the I_C state and reopening currents were not observed upon repolarization. Beck *et al.* (2002) expanded upon this model in their analysis of the effects of KChIP1 on Kv4.1 and Kv4.3. The model (Fig. 13*A*) proposes that Kv4.1/4.3 inactivation is due to a concerted action of the Kv4 α subunit N- and C-termini and interactions between the distal region of S6 and the S4–S5 loop. Two assumptions of this model are: (i) inactivation from the open state, mediated by the N-terminus, kinetically corresponds to the fast time constant, τ_{fast}, of inactivation; and (ii) inactivation from the closed state, mediated by conformational changes near the internal mouth of the pore, kinetically corresponds to the slow time constant(s), τ_{slow}, of inactivation. It is also proposed that KChIP1 binds and immobilizes the N-terminus leading to a slowing of open-state inactivation. This would result in less steric hindrance around the internal mouth of the pore, favouring closed-state inactivation and lowering the energy barrier for recovery. This model also predicts that minimal to no reopening currents would be generated upon membrane hyperpolarization. While this model could reasonably reproduce Kv4 activation and inactivation kinetics during depolarizing voltage clamp step pulses, it was not demonstrated that it could reproduce recovery kinetics at hyperpolarized potentials.

Kv4.3/KChIP2 isoform model. Similar to the allosteric models, it predicts prominent closed state inactivation (Patel *et al.* 2004). However, it proposes that inactivation, measured as a biexponential process, can occur from both preactivated closed states and the open state by a second, obligatorily coupled inactivation pathway that is at least

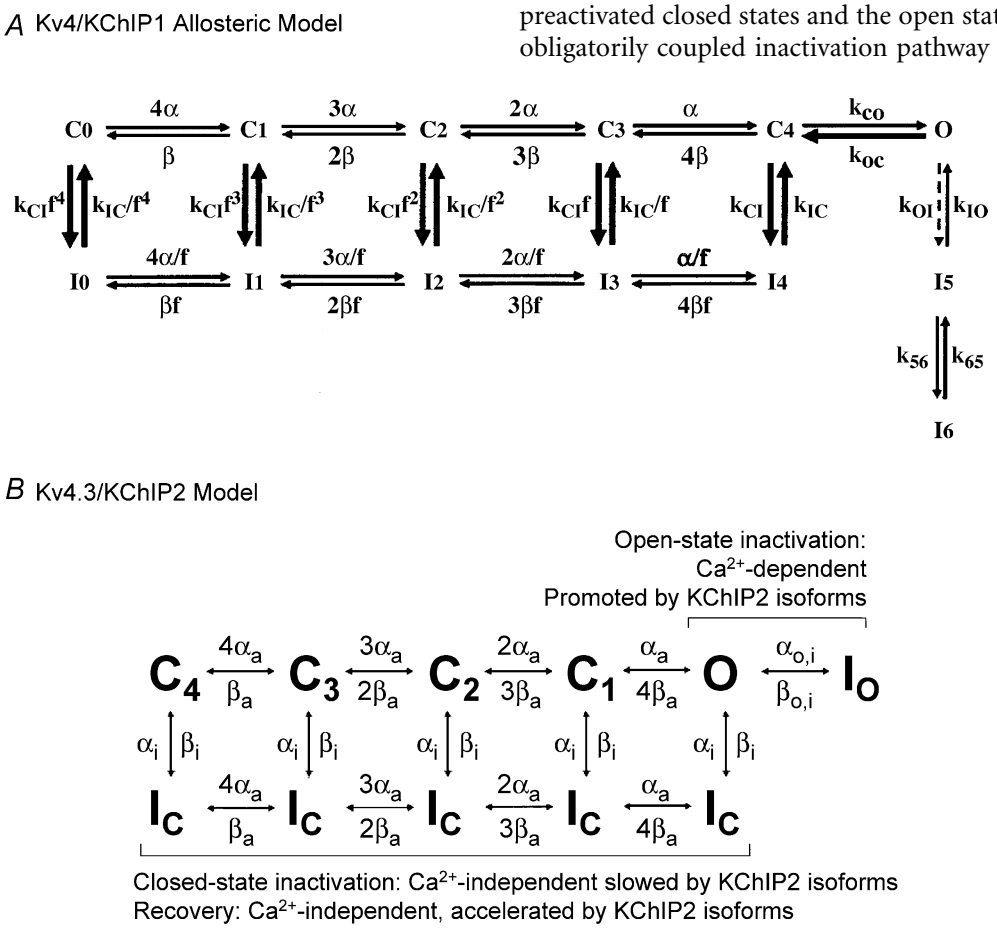

Figure 13. Proposed Kv4/KChIP gating models
A, Kv4/KChIP1 allosteric model. C, closed states; I, inactivated states; and O, open states. Rate constants α and β are assumed to be exponentially dependent upon voltage, while the transitions between C_4 and O are weakly voltage dependent or voltage independent. The transition from C_4 to O is also reversed biased to favour accumulation in inactivated closed states. Channels can inactivate from either open or closed states; however, along with the reverse biasing of the C_4 to O transition, the 'allosteric factor', f, further biases the voltage dependence of inactivation to progressively favour inactivation from later closed states. Transitions that are hypothesized to be favoured by KChIP1 are indicated by the bolder arrows. *B*, Kv4.3/KChIP2 model. KChIP2 is hypothesized to slow closed state inactivation and promote the obligatorily coupled open-inactivated state I_O, thus resulting in prominent reopening currents upon membrane hyperpolarization. This model also incorporates the effects of varying $[Ca^{2+}]_i$. Models from: *A*, Beck *et al.* (2002); *B*, Patel *et al.* (2004).

partially absorbing (Fig. 13*B*). The assignment of time constants is opposite to that of the allosteric models: closed state inactivation transitions are assigned to τ_{fast} and open state inactivation transitions to τ_{slow}.

This model predicts that KChIP2 isoforms slow closed state inactivation. They also promote/accelerate the slower component of inactivation via an obligatorily coupled open state inactivation process. As a result, in the presence of KChIP2 isoforms: (i) at depolarized potentials inactivation becomes slowed and approaches single exponential behaviour; and (ii) upon membrane repolarization reopening currents are promoted. The latter prediction is supported by the recent observations of Gebauer *et al.* (2004) demonstrating reopening of Kv4.2 channels upon membrane repolarization. This Kv4.3/KChIP2 model is also unique in that it incorporates $[Ca^{2+}]_i$ dependency: regulation of closed state transitions is $[Ca^{2+}]_i$ independent, while regulation of the slower, obligatorily coupled open state transition(s) is $[Ca^{2+}]_i$ dependent (Patel *et al.* 2002*b*, 2004). The predictions of this model have yet to be quantitatively tested.

Outer pore collapse model. This model (Eghbali *et al.* 2002) proposes the existence of a high affinity ($K_d < 2$ mM) K^+-selective modulatory site within the extracellular Kv4.x pore vestibule. Due to its high affinity, this site is assumed to be saturated at normal (~2 mM) $[K^+]_o$. This model further proposes that: (i) binding of K^+ to the neighbouring high affinity selectivity filter within the pore (Heginbotham *et al.* 1994; Doyle *et al.* 1998; Jiang *et al.* 2003*b*) promotes electrostatic interactions between K^+ ions in the external modulatory site; and (ii) the selectivity filter can bind K^+ ions in the closed state. These characteristics would result in destabilization of the modulatory site by electrostatic interactions and allow inactivation from closed states. Thus, this model predicts that raising $[K^+]_o$ (> 2 mM) would have no effects on Kv4 inactivation or recovery. While this is an interesting proposal, it does not account for the observations that increasing $[K^+]_o$ well above 2 mM produces concentration-dependent modulatory effects on Kv4 gating kinetics (Jerng *et al.* 1999; Campbell, Patel & Strauss, 2002; Wang *et al.* 2004).

Structural–functional insights

In this section we focus on recent advances made in structure–function relationships governing Kv4 channels. For readers interested in similar advances made in Shaker and Kv1.4 channels we suggest the excellent review by Sokolova (2004).

HPTX/PaTX structures. HPTXs and PaTXs inhibit Kv4 channels not by occluding the pore but rather by modifying gating properties. Thus, similar to the effects originally described for hanatoxin on Kv2.1 channels, these toxins should be referred to as Kv4 'gating modifiers' rather than 'blockers' (Swartz & MacKinnon, 1997). Gating modification is hypothesized to occur via an external site(s) that is accessible when Kv4 channels are in the closed state(s) (Diochot *et al.* 1999; Chagot *et al.* 2004). Depolarization results in reduced accessibility, affinity and/or disruption of the toxin binding site(s) due to conformational changes of the tetrameric α subunit complex.

Insights into the feasibility of this proposal have recently been provided by determination of the solution structures of HPTX2 and PaTX1 (Bernard *et al.* 2000; Diochot *et al.* 1999). Both toxins belong to a larger family of peptide toxins that display an 'inhibitory cysteine knot' (ICK) motif (Norton & Pallaghy, 1998). The ICK motif consists of a triple-stranded, antiparallel β-sheet ring structure stabilized by a 'cysteine knot' composed of six cysteine residues. This produces an embedded ring structure consisting of three β-sheets, the first and second of which are linked by disulphide bonds with the protein backbone and 'threaded' with a third disulphide bond between the third sheet and the backbone (Fig. 14*B*). This motif results in a highly stable structure, with the formation of a hydrophobic core from which only short loops emerge. (A good introduction to cysteine knots and their variations in different peptide toxins can be found at the Cyclotide webpage (www.cylcotide.com) and the KNOTTIN website database links (http://knottin.cbs.cnrs.fr/).

Molecular modelling studies suggest that HPTX2 and PaTX1 display very similar interaction surfaces with their Kv4 receptor(s) (Bernard *et al.* 2000; Shiau *et al.* 2003; Diochot *et al.* 1999). Due to overall charge distribution, electrical anisotropy results in a predicted dipole moment emerging through the β-sheet near central Lys 26 in PaTX1 and central Lys 27 in HPTX2 (Fig. 14*C*, upper panel). Around these central lysines are both a basic residue and an aromatic cluster (Fig. 14*C*, lower panel). The dipole is thus associated with a 'hydrophobic patch domain'. Toxin selectivity would arise from a combination of hydrophobic and electrostatic interactions with the Kv4 receptor site(s), the latter presumably being extracellularly accessible regions of S4 (Shiau *et al.* 2003; Chagot *et al.* 2004). However, verification of these modelling proposals awaits further experimental evidence (for detailed discussions of this subject please see: Shiau *et al.* 2003; Lee & MacKinnon, 2004; Ruta & MacKinnon, 2004).

KChIP1 crystal structure. KChIP1 is composed of 10 α helices, with helices H1–H5 forming an N-terminal 'lobe' and helices H6–H10 forming a C-terminal 'lobe' (Fig. 15). Thus, the overall crystal structure of KChIP1 has two 'faces', one hydrophilic (containing functional EF-hands 3 and 4) and the other hydrophobic. The Kv4 N-terminus binds in the groove of the hydrophobic face (Zhou *et al.* 2004; Scannevin *et al.* 2004).

Interestingly, the loop domain in KChIP2d (amino acids 14–21), which Patel *et al.* (2002*b*) demonstrated to be involved in regulation of Kv4.3 recovery, appears to be a highly flexible structure, as suggested by the fact that Zhou *et al.* (2004) were unable to structurally resolve the corresponding region in the KChIP1 crystal structure (Fig. 15*A* and *B*). Could high conformational flexibility provide a basis for allowing the KChIP loop domain to regulate Kv4.3 recovery kinetics independently of EF-hand- mediated conformational changes (Patel *et al.* 2002*b*, 2004)?

Zhou *et al.* (2004) also propose that Ca^{2+}-binding to EF hands 3 and 4 promotes conformational changes that fully expose the hydrophobic pocket required for KChIP1 binding to the Kv4.2 N-terminus. Without these Ca^{2+}-mediated interactions binding would be much less efficient. However, KChIPs with mutated EF-hands still coimmunoprecipitate with Kv4 α subunits (An *et al.* 2000) and maintain regulatory effects on Kv4.3 recovery kinetics (Patel *et al.* 2002*b*). These results suggest that if the binding interactions proposed by Zhou *et al.* (2004) are weaker in the absence of Ca^{2+} or presence of mutated EF-hands, then there must be additional unresolved interactions between KChIPs and Kv4 channel regions to maintain the observed binding and regulatory effects.

Zhou *et al.* (2004) also reported that under their experimental conditions (introduction of non-physiological covalent bonds between binding domains of KChIP1 and Kv4.2) KChIP1 forms dimers. To account for the 4 : 4 stoichiometry of the Kv4.2–KChIP2 complex (Kim *et al.* 2003), they propose that a pair of KChIP dimers bind to the Kv4 tetrameric complex. As Zhou *et al.* (2004)

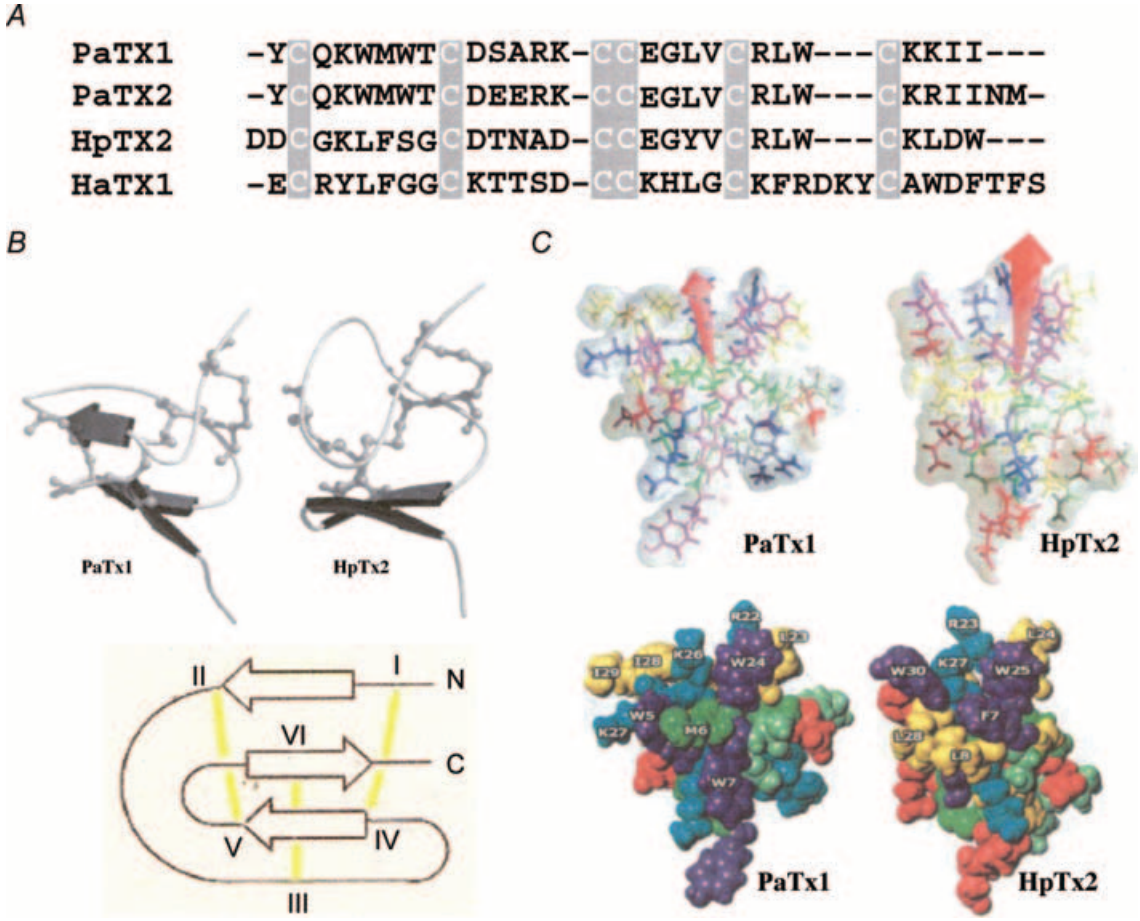

Figure 14. Spider toxins
A, amino acid sequence alignments of PaTXs and HPTXs. Cysteine residues involved in ICK motif formation are indicated by grey boxes. *B*, the ICK motif is schematically illustrated in the lower panel. Roman numerals *I–VI* correspond to the cysteine residues indicated in *A*. The upper panels illustrate MOLESCRIPT representations of the predicted solution structures of PaTX1 and HPTX2. *C*, predicted solution structures. The upper panels illustrate putative interaction surfaces, with the orientation of the predicted dipole moments emerging from the hydrophobic patches indicated by red arrows. CPK representations are illustrated in the lower panels in the same orientation. Colour coding: polar uncharged residues, green; basic residues, blue; acidic residues, red; aromatic residues, purple; aliphatic residues, yellow. Data modified from Chagot *et al.* (2004) (with permission from Cold Spring Harbor Laboratory Press) and the Cyclotide webpage (with permission from David Craik).

point out, this leads to a potential symmetry mismatch between KChIPs and Kv4 channels. However, Chang *et al.* (2003) have reported that KChIP1 displays a tendency to form dimers in the absence of metal ions and tetramers in the presence of metal ions. Thus, the issues of KChIP dimerization (representative of the native complex within LV myocytes?), dependence upon $[Ca^{2+}]_i$ and number of KChIPs bound per Kv4.2/4.3 α subunit are still unclear.

Kv4.2 N-terminus structure. Bähring *et al.* (2001*b*) initially demonstrated that a stretch of hydrophobic amino acids in the distal N-terminus of Kv4.2 was involved in KChIP binding. Subsequently, Scannevin *et al.* (2004) determined the crystal structure of the Kv4.2 T1 (tetramerization) domain. Two regions in the Kv4.2 N-terminus, residues 7–11 and residues 71–90, were found to be involved in KChIP1 interactions. Region 7–11 contains mainly hydrophobic residues, while region 71–90 forms an extended hydrophilic 'docking loop'. Mutagenesis analysis revealed that the amino acid 71–90 docking loop confers KChIP-binding to Kv1.2 (which does not bind KChIPs under native conditions). In this region, the mutation F74R was most significant in reducing the effects of KChIP1, suggesting that aromatic interactions may be involved.

Three-dimensional (EM) structure of the Kv4.2/KChIP2 channel complex. Using negative stain electron microscopy, Kim *et al.* (2004) have determined the three-dimensional structure (21 Å resolution) of the

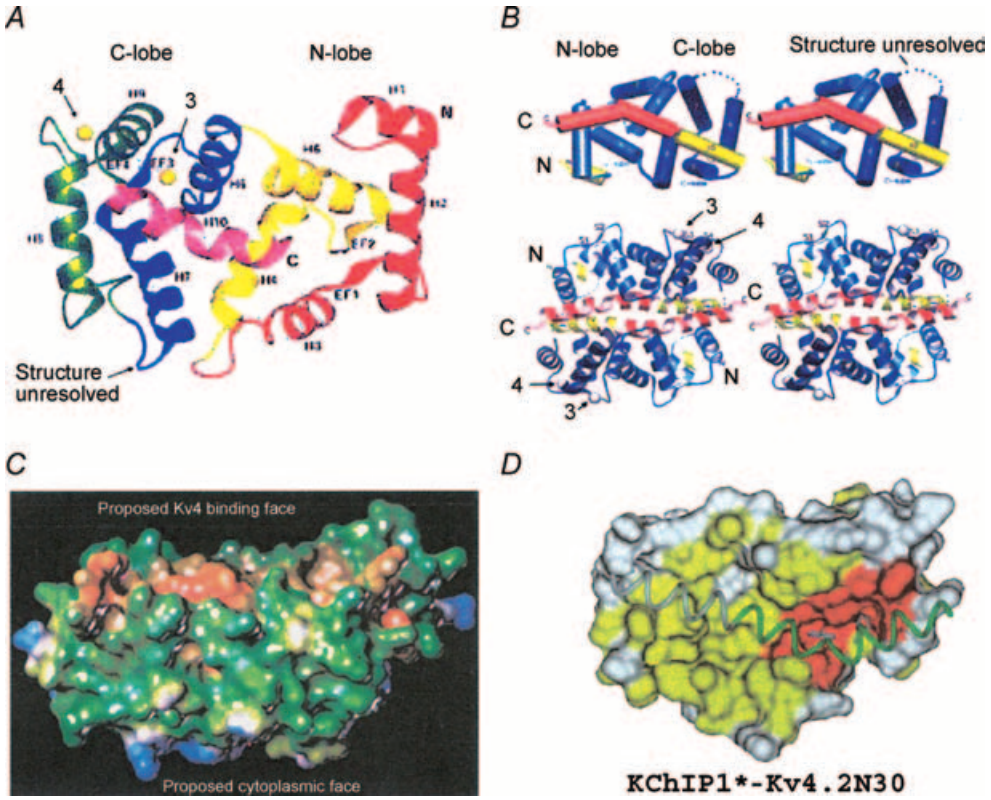

Figure 15. KChIP1 crystal structure
A, KChIP1 ribbon representation. EF-hands designated EF1–4, Ca^{2+} ions as yellow spheres and α helices as H1–H10. Arrows 3 and 4 point to the Ca^{2+} ions bound to EF-hands 3 and 4, respectively. *B*, upper panel: stereo views of cylinder model of KChIP1 monomer, with Kv4.2 N-terminus in orange. Note that the structurally unresolved region between H7 and H8 (indicated as a break in *A* and a dotted line in *B*) corresponds to the 'recovery loop' region originally mutated by Patel *et al.* (2002*b*). Lower panel: stereo view of ribbon model of the KChIP1-Kv4.2 N30 dimeric complex, rotated 90 deg around the horizontal axis from upper panel view. Ca^{2+} ions bound to EF-hands 3 and 4 indicated as grey spheres. N and C indicate the N- and C-terminus of each individual KChIP. Arrows 3 and 4 designate Ca^{2+} ions bound to EF-hands 3 and 4, respectively. *C*, lipophilic (Kv4-binding) and hydrophilic (cytoplasmic-orientated) faces of KChIP1. Surfaces have been colour coded to indicate lipophilicity, with brown being highly lipophilic and blue highly hydrophilic. *D*, surface map structure of the KChIP1 hydrophobic binding pocket and its interaction with the Kv4.2N30 construct (green ribbon model; see Zhou *et al.* 2004 for further details). Colour coding of surface residues: polar residues, grey; non-polar residues, yellow. Red residues display sequence homology to other NCS proteins. Figures from: *A* and *C*, Scannevin *et al.* (2004) reproduced with permission from Elsevier; *B* and *D*, Zhou *et al.* (2004) reproduced with permission from Elsevier.

Kv4.2/KChIP2 complex. Similar to Shaker (Sokolova *et al.* 2001), Kv4.2 has a 'hanging gondola' held below the transmembrane pore by four N-terminal columns (Fig. 16). Kim *et al.* (2004) also modelled the structures of Shaker (Sokolova *et al.* 2001) and frequenin (Bourne *et al.* 2001) superimposed on the Kv4.2–KChIP2 complex. This modelling revealed that, in marked contrast to Shaker, the Kv4.2–KChIP2 complex has four 'peripheral columns' that extend from the membrane-bound Kv4.2 α subunits to the cytosolic regions where KChIP2 molecules bind to the Kv4.2 N-termini. This model predicts that KChIPs extend the gondola platform laterally to meet with the four peripheral columns.

While the identity of the peripheral columns has yet to be determined, Kim *et al.* (2004) speculate that they correspond to the C-termini of Kv4.2 α subunits. This is an appealing proposal: could the predicted close proximity of KChIPs and the Kv4 C-termini allow transduction of KChIP-mediated effects between N- and C-termini, and thus transduction of these effects to other physically distant regions of the α subunit? And is the absence of the four peripheral columns in Shaker a physical basis for some of the functional differences between Shaker and Kv4 channels?

It is also interesting to note that the Kv4.2 channel preparation used by Kim *et al.* (2004) contained no free Ca^{2+}. Might the KChIPs in the derived three dimensional structure have Ca^{2+}-free EF-hands? If this is the case, then could the Kv4 C-terminus serve as another Ca^{2+}-independent binding site for KChIP-mediated interactions, and could these interactions be responsible for Ca^{2+}-independent regulation of Kv4.3 recovery kinetics (Patel *et al.* 2002*b*, 2004)? Thus, while the Kv4 N-terminal T1 domain may help maintain Kv4–KChIP interactions, it is possible that there may be even stronger interactions between KChIPs and the Kv4.2/4.3 C-terminus.

Molecular models of Kv channel activation. While no Kv4 α subunit has yet been crystalized, the crystal structure of KvAP, a voltage-dependent K^+ channel from the thermolphilic archaebacterium *Aeropyrum permix*, has been determined (Jiang *et al.* 2003*b*,*c*). However, this pioneering work has led to a debate over the physical mechanisms governing Kv channel activation, with three major models having been proposed. (For readers interested in detailed discussions the following are excellent sources: Bezanilla, 2000, 2002; Gandhi & Isacoff, 2002; Bezanilla & Perozo, 2003; MacKinnon, 2003; Laine *et al.* 2003, 2004; Blaustein & Miller, 2004; Cuello *et al.* 2004).

Activation Model 1: 'sliding helix or corkscrew model'. This is the classic model of voltage-dependent channel gating (Fig. 17*A*). Recent evidence in its support comes from histidine scanning and LRET and FRET imaging (Starace *et al.* 1997; Cha *et al.* 1999; Glauner *et al.* 1999; Starace & Bezanilla, 2001). The major assumptions of this model are that: (i) the transmembrane segment S4, which contains positively charged arginines at approximately every third residue, is completely surrounded by a proteinaceous 'activation canal'; (ii) S4 lies close to, and may interact with, the pore domain; and (iii) upon membrane depolarization S4 moves through the activation canal towards the extracellular surface as a rigid rod via

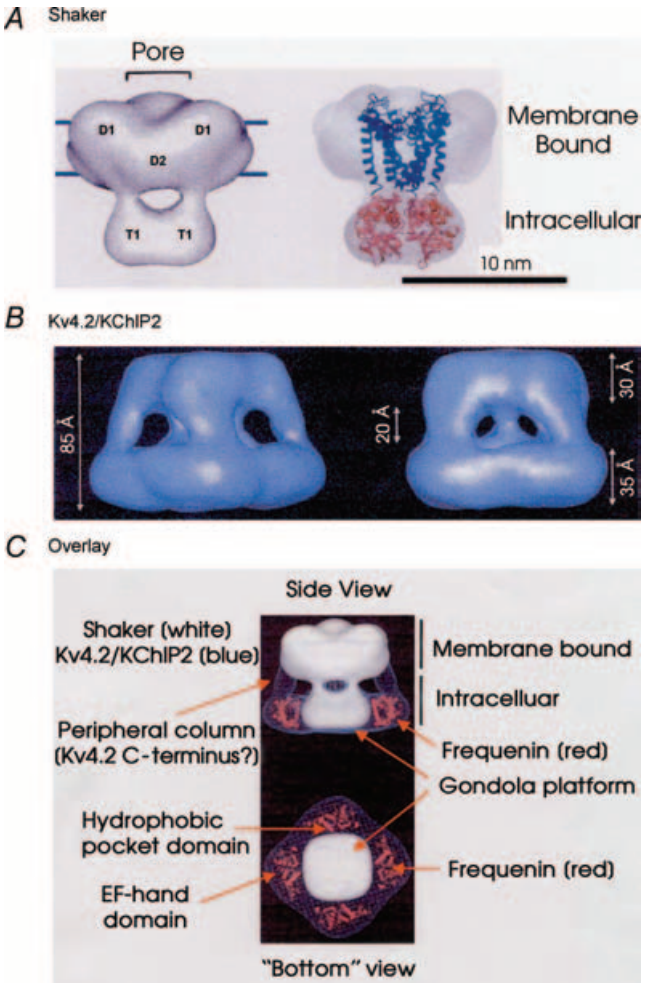

Figure 16. Three dimensional (electron microscopic (EM)) structures of Shaker and Kv4.2/KChIP2
A, Shaker channel. The left panel illustrates the 3D structure of the homotetrameric Shaker channel. D1 and D2 are subdomains embedded within the membrane and T1 is the tetramerization domain. The right panel is an overlay/docking of the crystal structures of the T1 tetramer (red) and the KcsA channel (blue). *B*, 3D EM structure of Kv4.2/KChIP2. The left panel illustrates a side view, while the right panel is a side view rotated 45 deg along the central axis of symmetry. *C*, EM structure of Shaker (white) overlaid on the Kv4.2/KChIP2 complex structure (blue mesh). The upper panel illustrates a side view (only two frequenin molecules (red) are illustrated) while the lower panel shows a 'bottom' view. Note the peripheral columns (Kv4.2 C-termini?) in the Kv4.2/KChIP2 complex that are absent in Shaker. Four frequenin molecules will only fit into the structure with their hydrophobic pockets facing the gondola platform thus exposing their hydrophilic EF-hand faces towards the cytosol. *A*, modified from Sokolova (2004) with permission; *B*, reproduced from Kim *et al.* (2004) with permission from Elsevier; *C*, modified from Kim *et al.* (2004) with permission from Elsevier.

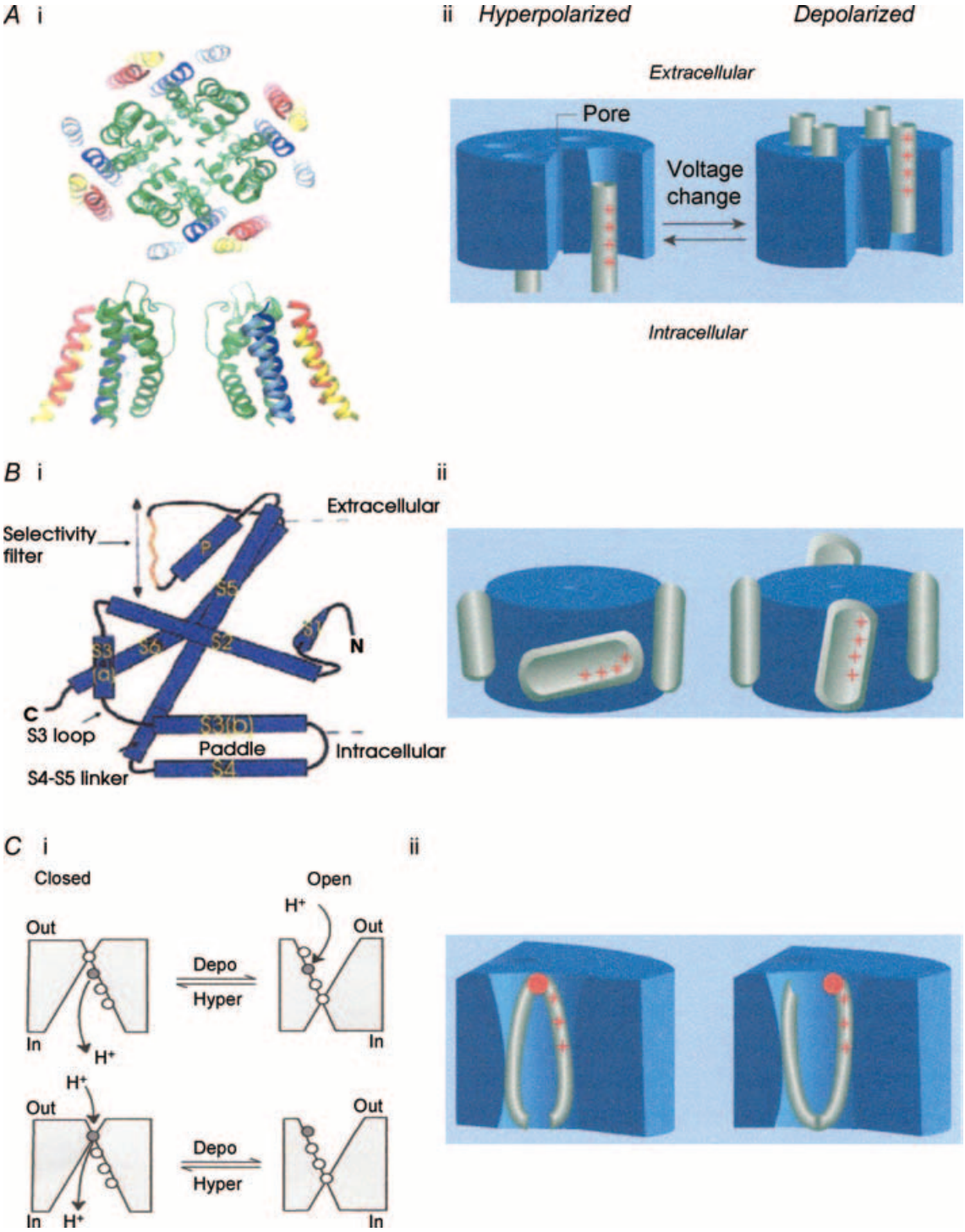

Figure 17. Kv channel activation models
A, helical-corkscrew model. S4 is hypothesized to be located next to, and potentially interacting with, the pore domain. *i*, upper panel: Shaker channel model viewed 'down' from the extracellular side. Domains colour coded as follows: S1, light blue; S2, yellow; S3, red; S4, dark blue; pore domain, green. *Lower panel*: Side view only showing 2 α subunits for clarity. *ii*, schematic representation of S4 movement in response to membrane depolarization. *B*, voltage-sensor paddle model. *i*, KvAP crystal structure (1 α subunit), channel closed state. The S3(b)–S4 voltage-sensor paddle lies parallel to the intracellular membrane surface and is located on the periphery of the channel. *ii*, upon membrane depolarization the paddles move ~20 Å perpendicular into the membrane, thus exposing to the extracellular environment amino acids in S3(b)–S4 that are either intracellular or embedded in the membrane in the closed state. *C*, carrier-like model: hypothesized Shaker S4 gating pore. *i*, schematic of proton

either sliding or corkscrewing through the gating pore (Fig. 17*Aii*).

Activation Model 2: 'voltage-sensor paddle model'. This model (Fig. 17*B*) is based upon the crystal structure of KvAP (Jiang *et al.* 2003*b*,*c*). The structure of KvAP segments S5 and S6, which form the pore and selectivity filter, were found to be very similar to the crystal structure of KcsA, a two transmembrane domain K^+ channel from *Streptomyces lividans* (Doyle *et al.* 1988). However, Jiang *et al.* (2003*b*) concluded that the structure of the voltage sensor was very different from that predicted by the helical corkscrew model: they proposed that segments S3 and S4 were located at the channel's *outer* perimeter. The second helix in S3, S3(b), and the amino terminal half of the traditionally defined S4 segment were found to form a hydrophobic helix-turn-helix structure termed the 'voltage-sensor paddle'. The S3 loop and S4–S5 linker provide flexibility, allowing the paddle to adopt more than one conformation. In the closed state, the S4 helices of the paddle of each α subunit are near the intracellular membrane surface, perpendicular to the pore axis, and are loosely attached to the pore domain. Upon membrane depolarization, the paddles move ∼20 Å perpendicular into the membrane, opening the channel by pulling on the S4–S5 linkers.

The major point of debate in this model is the proposal of S3b–S4 paddles existing on the *outer* perimeter of the channel and that the corresponding arginines would be exposed to the lipid environment of the membrane. No S4 gating pore is predicted. Arguments have been made that the KvAP structure may have been altered by detergents employed in its isolation, use of FAB fragments and/or crystal-packing forces (see discussions in Laine *et al.* 2003, 2004; Blaustein & Miller, 2004; Birnbaum *et al.* 2004). But the magnitude of such distortions is unclear. Furthermore, electron microscopic analysis (10.5 Åresolution) of KvAP in the *open* conformation suggests that the voltage-sensor paddles are near the extracellular surface and located at the protein–lipid interface (Jiang, Wang & MacKinnon, 2004).

Activation Model 3: 'gating pore' or 'transporter models'. These models do not incorporate a gating paddle but do incorporate many of aspects of the sliding/corkscrew helix model. However, these models propose that S4 is located at the periphery of the channel and is only partially surrounded by a proteinaceous 'gating pore'. The polar protein walls of the gating pore (provided by transmembrane helices S2 and S3 and the pore domain helices) are hypothesized to insulate the S4 arginines from lipids. Accessibility scanning measurements indicate that, upon depolarization, nine residues in S4 move from an inaccessible location, presumably within the gating pore, to a position that is accessible to the extracellular solution, a movement that corresponds to 13.5 Å of axial length of an α helix (Larsson *et al.* 1996; Mannuzzu *et al.* 1996; Baker *et al.* 1998; Schönherr *et al.* 2002). FRET measurements further suggest a ∼180 deg helical rotation (Cha *et al.* 1999; Glauner *et al.* 1999). The gating pore would thus be ∼13.5 Å long, contain water-filled vestibules at both of its ends, and would focus the transmembrane electric field on a small sequence of S4 within the narrow part of the gating pore (Fig. 18*A*).

Original support for this model (Fig. 17*C*) came from fluorescent measurements on Shaker channels indicating that S4 moved less than 2 Å in response to membrane depolarization (Cha *et al.* 1999). This model (Starace & Bezanilla, 2004) differs from the previous two models because it proposes that Kv channel activation occurs through a transporter-like mechanism. The model is based upon results obtained from Shaker channels where the first outermost arginine in S4 was mutated to histidine. This mutation results in production of a steady transmembrane proton current, conducted through the S4 gating pore, when the channel is in the closed-state (Starace & Bezanilla, 2004). Consistent with the gating pore hypothesis, in the closed-state protons can access the single histidine in S4 from *both* the extracellular and intracellular solutions. This implies that the gating pore focuses the transmembrane voltage gradient across the distance of a *single* S4 side chain residue! As a result, in response to membrane depolarization S4 moves only a few angstroms at most (in contrast to either the helical corkscrew or paddle models, which predict that S4 moves ∼13–20 Å perpendicular to the cell membrane).

conduction through the S4 gating pore based upon mutagenic replacement of S4 R365 by histidine. Upper panel: R365H mutant (indicated as grey sphere). Conformational changes underlying proton transport. In the presence of an inward proton gradient the R365H channel transports one proton per channel open-to-closed cycle. Lower panel: R362H mutant (indicated as grey sphere). Internal and external protons have simultaneous access to the histidine only when the channel is in the closed conformation allowing proton current flow only when the channel is closed. *ii*, schematic representation. The R362H mutation is indicated in red. In the closed conformation, a very narrow gate is formed that separates the extracellular and intracellular surfaces. This 'focuses' the transmembrane electric field over a very short distance of essentially one amino acid residue. *Ai*, fromLaine *et al.* (2003) with permission from Elsevier; *Bi*, modified from Jiang *et al.* (2003*b*) reprinted by permission from Nature, © 2003 Macmillan Publishers Ltd (http://www.nature.com/); *Ci*, from Starace & Bezanilla (2004) reprinted by permission from Nature, © 2004 Macmillan Publishers Ltd (http://www.nature.com/); *Aii*, *Bii* and *Cii*, Blaustein & Miller (2004) reprinted by permission from Nature, © 2004 Macmillan Publishers Ltd (http://www.nature.com/).

Further evidence for the existence of the S4 gating pore in Shaker has been provided by Tombola *et al.* (2005). These investigators demonstrated that when the first arginine in S4 was replaced with smaller amino acids, a manoeuvre that removed the guanidium group of arginine, a high conductance cation-selective pathway was formed within the putative S4 gating pore when the channel was in the resting state(s). This current was designated the 'omega current' to distinguish it from the conventional K^+-selective 'alpha current' that normally flows through the selectivity filter/pore domain of the open channel. The omega current, which could be blocked by Mg^{2+}, was supported by guanidium ions, consistent with the hypothesis that arginine residues move through the gating pore during channel activation. These results appear to be inconsistent with the gating paddle model. It was thus proposed that under normal conditions activation of S4 involves 'ratcheting' movements between intermediate conformational states where each of the arginines successively occupies the gating pore, thereby occluding ion conduction through the gating pore as the channel activates (Tombola *et al.* 2005; Fig. 18).

In summary, while there is universal consensus on the role of S4 in Kv channel activation, there is considerable debate on the underlying molecular mechanisms. Also, when considering these models, it should be kept in mind

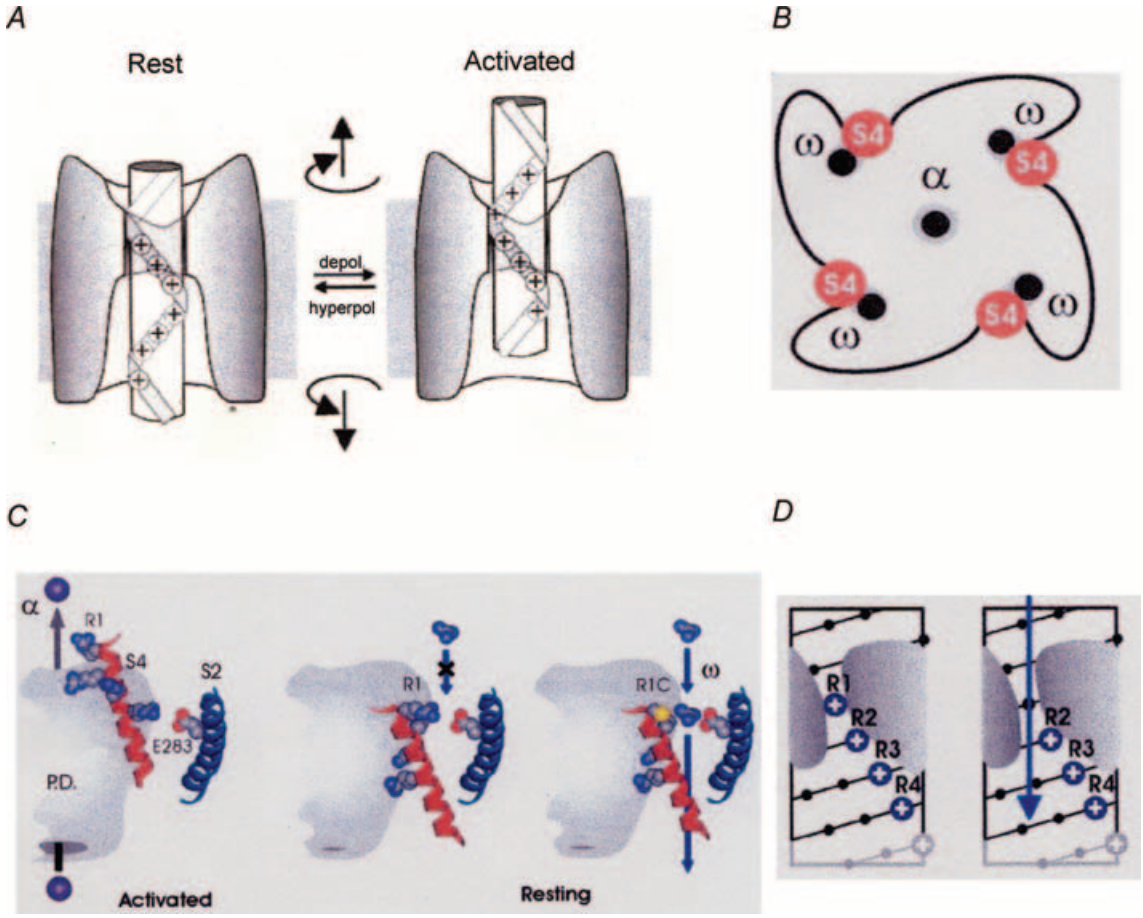

Figure 18. Shaker channels: hypothesized S4 gating pore
A, schematic of voltage-dependent S4 movement within the gating pore. *B*, hypothesized locations of S4, gating pore domains (ω) and the channel K^+ pore selectivity/conduction domain (α). S4 arginines are hypothesized to face the polar proteinaceous walls of the gating pore formed by S2, S3 and the K^+ pore helices. *C*, proposed 'ratcheting' interactions between S4 arginines and S2 E283. Cartoons illustrate relative positions of S4 and S2 in the resting and activated states. At rest, R1 blocks ion conduction through the gating pore. Upon depolarization, R1, R2, R3 and R4 each successively 'ratchet' through the gating pore, with each intermediate state blocking ion conduction. PD, channel pore domain; α, K^+ current through the channel pore; ω, guanidium current flow through the gating pore in the presence of mutation R1C. *D*, mutation of R1 to smaller amino acids (guanidium group removal) unblocks the gating pore at rest, leading to flow of a cation-selective 'omega current' (blue arrow). Figures from: *A*, Gandhi & Isacoff (2002) by copyright permission of The Rockefeller University Press; *B*, *C* and *D*, Tombola *et al.* (2005) reproduced with permission from Elsevier.

that there are differences in the sequences of S3b–S4 of KvAP, Shaker and Kv4.2/4.3. For example, the first arginine in the S4 segment of Shaker is replaced by a valine in Kv4.2. Thus, might there be differences in the gating pores of Shaker verus Kv channels? And, on a more fundamental level, might there also be differences in the basic structural mechanisms underlying activation of Kv channels in prokaryotes *versus* eukaryotes?

Concluding remarks

We have attempted to summarize what we feel are the major advances that have been made in our understanding of LV I_{to} phenotypes. We have emphasized important functional differences between $I_{to,fast}$ and $I_{to,slow}$ and differences among species in the transmural LV free wall distributions of these two I_{to} phenotypes. We have also reviewed those areas where at present we lack understanding of underlying mechanisms. At the molecular level, while analysis of Shaker channels has provided insight into molecular mechanisms governing gating of Kv1.4-mediated $I_{to,slow}$, it is now clear that these mechanisms are not always applicable to Kv4.2/4.3 channels, particularly with regard to inactivation and recovery. At the cellular level, particular areas that we feel need further investigation are: (i) the role of normal alterations in $[Ca^{2+}]_i$ on $I_{to,fast}$ kinetics (given that KChIPs provide a means for Ca^{2+}-dependent regulation of Kv4 channels) and its predicted behaviour during an LV myocyte action potential; (ii) the role of $I_{to,slow}$ in species where this phenotype is prominent in LV endo myocytes; (iii) kinase-dependent modulation of $I_{to,fast}$ (obligatory KChIP2 involvement?) and $I_{to,slow}$; and (iv) determination of protein expression patterns of different regulatory subunits across the LV free wall and the functional consequences of such gradients. These considerations then need to be incorporated into mathematical models of LV electrical activity. Finally, the contributions of different LV I_{to} phenotypes to both repolarization gradients and arrhythmic conditions need to be evaluated.

Note added in proof

During the production process of this review four articles have appeared which have direct relevance to issues that have been discussed: 1) Radicke *et al.* (2005; *J Physiol.* **565.3**, 751–756) have cloned DPP6 from human ventricle and demonstrated that it regulates Kv4.3 gating kinetics; 2) Long, Campbell & MacKinnon (2005*a*,*b*; *Science* **309**, 897–903, 903–908) have determined the crystal structure of the mammalian Shaker family Kv1.2 channel in the open state; and 3) Wang *et al.* (2005; *Biophys. J.* [epub ahead of print]) have both independently reported Kv4.3 reopening currents (Patel *et al.*, 2004) and, using mathematical modelling, have quantitatively demonstrated that proposed allosteric Kv4 channel gating models (e.g. Beck *et al.*, 2002; see Figure 13.A) cannot successfully reproduce the overall gating characteristics of Kv4.3 channels.

References

Aldrich RW (1981). Inactivation of voltage-gated delayed potassium current in molluscan neurons. A kinetic model. *Biophys J* **36**, 519–532.

An WF, Bowlby MR, Betty M, Cao J, Ling HP, Mendoza G, Hinson JW, Mattsson KT, Strassle RW, Trimmer JS & Rhodes KJ (2000). Modulation of A-type potassium channels by a family of calcium sensors. *Nature* **403**, 553–556.

Anderson AE, Adams JP, Qian Y, Cook RG, Pfaffinger PJ & Sweatt JD (2000). Kv4.2 phosphorylation by cyclic AMP-dependent protein kinase. *J Biol Chem* **275**, 5337–5346.

Antzelevitch C, Zygmunt AC & Dumaine R (2003). Electrophysiology and pharmacology of ventricular repolarization. In *Cardiac Repolarization*, ed. Gussak I & Antzelevitch C, pp. 63–89. Human Press Inc., Totowa, NJ, USA.

Archer SL & Rusch NJ (2001). *Potassium Channels in Cardiovascular Biology*. Kluwer Academic/Plenum Publishers, New York.

Bähring R, Boland LM, Varghese A, Gebauer M & Pongs O (2001*a*). Kinetic analysis of open- and closed-state inactivation transitions in human Kv4.2 A-type potassium channels. *J Physiol* **535**, 65–81.

Bähring R, Dannenberg J, Peters HC, Leicher T, Pongs O & Isbrandt D (2001*b*). Conserved Kv4 N-terminal domain critical for effects of Kv channel-interacting protein 2.2 on channel expression and gating. *J Biol Chem* **276**, 23888–23894.

Baker OS, Larrsson HP, Mannuzzu LM & Isacoff EY (1998). Three transmembrane conformations and sequence-dependent displacement of the S4 domain in shaker K^+ channel gating. *Neuron* **20**, 1283–1294.

Barry DM, Xu H, Schuessler RB & Nerbonne JM (1998). Functional knockout of the transient outward current, long-QT syndrome, and cardiac remodeling in mice expressing a dominant-negative Kv4 α subunit. *Circ Res* **83**, 560–567.

Bassani RA, Altamirano J, Puglisi JL & Bers DM (2004). Action potential duration determines sarcoplasmic reticulum Ca^{2+} reloading in mammalian ventricular myocytes. *J Phyisol* **559**, 593–609.

Beck EJ, Bowlby M, An WF, Rhodes KJ & Covarrubias M (2002). Remodeling inactivation gating of Kv4 channels by KChIP1, a small-molecular-weight calcium-binding protein. *J Physiol* **538**, 691–706.

Beck EJ & Corvarrubias M (2001). Kv4 channels exhibit modulation of closed-state inactivation in inside-out patches. *Biophys J* **81**, 867–883.

Bernard C, Legros C, Ferrat G, Bischoff U, Marquardt A, Pongs O & Darbon H (2000). Solution structure of HPTX2, a toxin from *Heteropoda venatoria* spider that blocks Kv4.2 potassium channel. *Protein Sci* **9**, 2059–2067.

Bers DM (2001). *Excitation-Contraction Coupling and Cardiac Contractile Force*, 2nd edn. Kluwer Academic Publishers, Dordrecht.

Bett GC & Rasmusson RL (2004). Inactivation and recovery in Kv1.4 K^+ channels: lipophilic interactions at the intracellular mouth of the pore. *J Physiol* **556**, 109–120.

Bezanilla F (2000). The voltage sensor in voltage-dependent ion channels. *Physiol Rev* **80**, 555–592.

Bezanilla F (2002). Voltage sensor movements. *J General Physiol* **120**, 465–473.

Bezanilla F & Perozo E (2003). The voltage sensor and the gate in ion channels. *Adv Protein Chem* **63**, 211–241.

Birnbaum SG, Varga AW, Yuan L-Y, Anderson AE, Sweatt JD & Schraeder LA (2004). Structure and function of Kv4-family transient potassium channels. *Physiol Rev* **84**, 803–833.

Blaustein RO & Miller C (2004). Shake, rattle or roll? *Nature* **427**, 499–500.

Bondarenko VE, Szigeti GP, Bett GC, Kim SJ & Rasmusson RL (2004). Computer model of action potential of mouse ventricular myocytes. *Am J Physiol* **287**, H1378–H1403.

Bourne Y, Dannenberg J, Pollmann V, Marchot P & Pongs O (2001). Immunocytochemical localization and crystal structure of human frequenin (neuronal calcium sensor 1). *J Biol Chem* **276**, 11949–11955.

Boyett MR, Honjo H, Lei M & Kodama I (2001). Transient outward K^+ current, i_{to}, in the sinoatrial node. *Cardiovascular Res* **52**, 519–520.

Brahmajothi MV & Campbell DL (1999). Heterogeneous basal expression of nitric oxide synthase and superoxide dismutase isoforms in mammalian heart. Implications for mechanisms governing indirect and direct nitric-oxide-related effects. *Circ Res* **85**, 575–587.

Brahmajothi MV, Campbell DL, Rasmusson RL, Morales MJ, Trimmer JS, Nerbonne JM & Strauss HC (1999). Distinct transient outward potassium current (I_{to}) phenotypes and distribution of fast-inactivating potassium channel alpha subunits in ferret left ventricular myocytes. *J General Physiol* **113**, 581–600.

Brahmajothi MV, Morales MJ, Liu S, Rasmusson RL, Campbell DL & Strauss HC (1996). *In situ* hybridization reveals extensive diversity of K^+ channel mRNA in isolated ferret cardiac myocytes. *Circ Res* **78**, 1083–1089.

Brunet S, Aimond F, Li H, Guo W, Eldstrom J, Fedida D, Yamada KA & Nerbonne JM (2004). Heterogeneous expression of repolarizing, voltage-gated K^+ currents in adult mouse ventricles. *J Physiol* **559**, 103–120.

Brunner M, Guo W, Mitchell GF, Buckett PD, Nerbonne JM & Koren G (2001). Characterization of mice with a combined suppression of $I_{(to)}$ and $I_{(K,slow)}$. *Am J Physiol* **281**, H1201–H1209.

Campbell DL, Patel SP & Strauss HC (2002). 'Anomalous' effects of varying $[K^+]_o$ on inactivation and recovery kinetics of ferret left ventricular I_{to}. *Biophys J* **82**, 1186.

Campbell DL, Qu Y, Rasmusson RL & Strauss HC (1993*a*). The calcium-independent transient outward potassium current in isolated ferret right ventricular myocytes. II. Closed-state reverse use-dependent block by 4-aminopyridine. *J General Physiol* **101**, 603–626.

Campbell DL, Rasmusson RL, Comer MB & Strauss HC (1995). The cardiac calcium-independent transient outward potassium current: kinetics, molecular properties, and role in ventricular repolarization. In *Cardiac Electrophysiology: from Cell to Bedside*, ed. Zipes DP & Jalife J, pp. 83–96. Saunders, Philadelphia.

Campbell DL, Rasmusson RL, Qu Y & Strauss HC (1993*b*). The calcium-independent transient outward potassium current in isolated ferret right ventricular myocytes. I. Basic characterization and kinetic analysis. *J General Physiol* **101**, 571–601.

Campbell DL, Rasmusson RL & Strauss HC (1992). Ionic current mechanisms generating vertebrate primary cardiac pacemaker activity at the single cell level: An integrative view. *Ann Rev Physiol* **54**, 279–302.

Campbell DL, Stamler JS & Strauss HC (1996). Redox modulation of L-type calcium channels in ferret ventricular myocytes. Dual mechanism regulation by nitric oxide and S-nitrosothiols. *J General Physiol* **108**, 277–293.

Campomanes CR, Carroll KL, Manganas LN, Hershberger ME, Gong B, Antonucci DE, Rhodes KJ & Trimmer JS (2002). Kv β subunit oxidoreductase activity and Kv1 potassium channel trafficking. *J Biol Chem* **277**, 8298–8305.

Carmeliet E & Vereecke J (2002). Ionic currents and action potentials in cardiac cells. In *Cellular Cardiac Electrophysiology*, pp. 95–117. Kluwer Academic Publishers, Boston.

Casis O, Iriarte M, Gallego M & Sanchez-Chapula JA (1998). Differences in regional distribution of K^+ current densities in rat ventricle. *Life Sci* **63**, 391–400.

Castellino RC, Morales MJ, Strauss HC & Rasmusson RL (1995). Time- and voltage-dependent modulation of a Kv1.4 channel by a β-subunit (Kvβ3) cloned from ferret ventricle. *Am J Physiol* **269**, H385–H391.

Cha A, Snyder GE, Selvin PR & Bezanilla F (1999). Atomic scale movement of the voltage-sensing region in a potassium channel measured via spectroscopy. *Nature* **402**, 809–813.

Chagot B, Escoubas P, Villegas E, Bernard C, Ferrat G, Corzo G, Lazdunski M & Darbon H (2004). Solution structure of Phrixotoxin 1, a specific peptide inhibitor of Kv4 potassium channels from the venom of the therapsid spider *Phrixotrichus auratus*. *Protein Sci* **13**, 1197–1208.

Chang L-S, Chen C-Y & Wu TT (2003). Functional implication with the metal-binding properties of KChIP1. *Biochem Biophys Res Commun* **311**, 258–263.

Chien KR (1999). *Molecular Basis of Cardiovascular Disease*. W. B. Saunders Company, Philadelphia.

Choi KI, Aldrich RW & Yellen G (1991). Tetraethylammonium blockade distinguishes two inactivation mechanisms in voltage-activated K^+ channels. *Proc Natl Acad Sci U S A* **88**, 5092–5095.

Clark RB, Bouchard RA, Salinas-Stefanon E, Sanchez-Chapula J & Giles WR (1993). Heterogeneity of action potential waveforms and potassium currents in rat ventricle. *Cardiovasc Res* **27**, 1795–1799.

Clark RB, Giles WR & Imaizumi Y (1988). Properties of the transient outward current in rabbit atrial cells. *J Physiol* **405**, 147–168.

Comer MB, Campbell DL, Rasmusson RL, Lamson DR, Morales MJ, Zhang Y & Strauss HC (1994). Cloning and characterization of an I_{to}-like potassium channel from ferret ventricle. *Am J Physiol* **267**, H1383–H139.

Craig TA, Benson LM, Venyaminov SY, Klimtchuk ES, Bajzer Z, Prendergast FG, Naylor S & Kumar R (2002). The metal binding properties of DREAM. Evidence for calcium-mediated changes in DREAM structure. *J Biol Chem* **277**, 10955–10966.

Cuello LG, Cortes DM & Perozo E (2004). Molecular architecture of the KvAP voltage-dependent K^+ channel in a lipid bilayer. *Science* **306**, 491–495.

Deal KK, England SK & Tamkum MM (1996). Molecular physiology of cardiac potassium channels. *Physiol Rev* **76**, 49–67.

de Bakker JMT & Opthof T (2002). Is the apico-basal gradient larger than the transmural gradient? *J Cardiovas Pharm* **39**, 328–331.

Decher N, Barth AS, Gonzalez T, Steinmyer K & Sanguinetti MC (2004). Novel KChIP2isoforms increase functional diversity of transient outward potassium current. *J Physiol* **557**, 761–772.

Decher N, Uyguner O, Scherer CR, Karaman B, Yüskelapak M, Busch AE, Steinmeyer K & Wollnik B (2001). hKChIP2 is a functional modifier of hKv4.3 potassium channels: cloning and expression of a short hKChIP2 splice variant. *Cardiovas Res* **52**, 255–264.

Deck KA & Trautwein W (1964). Ionic currents in cardiac excitation. *Pflugers Arch* **280**, 63–80.

Demo SD & Yellen G (1991). The inactivation gate of the Shaker K^+ channel behaves like an open-channel blocker. *Neuron* **7**, 743–753.

Deschênes I, DiSilvestre D, Juang GJ, Wu R, An WF & Tomaselli GF (2002). Regulation of Kv4.3 current by KChIP2 splice variants: a component of native cardiac I_{to}? *Circulation* **106**, 423–429.

Deschênes I & Tomaselli GF (2002). Modulation of Kv4.3 current by accessory subunits. *FEBS Lett* **528**, 183–188.

Diochot S, Drici MD, Moinier D, Fink M & Lazdunski M (1999). Effects of phrixotoxins on the Kv4 family of potassium channels and implications for the role of I_{to1} in cardiac electrogenesis. *Br J Pharmacol* **126**, 251–263.

Dixon JE & McKinnon D (1994). Quantitative analysis of mRNA expression in atrial and ventricular muscle of rats. *Circ Res* **79**, 659–668.

Dixon JE, Shi W, Wang H-S, MacDonald CYuH, Wymore R, Cohen IS & McKinnon D (1996). Role of the Kv4.3 potassium channel in ventricular muscle: a molecular correlate for the transient outward current. *Circ Res* **79**, 659–668.

Doyle DA, Cabral JM, Pfuetzner RA, Kuo A, Gulbis JM, Cohen SL, Chait BT & MacKinnon R (1998). The structure of the potassium channel: molecular basis of K^+ conduction and selectivity. *Science* **280**, 69–77.

Eghbali M, Olcese R, Zarei MM & Stefani E (2002). External pore collapse as an inactivation mechanism for Kv4.3 K^+ channels. *J Memb Biol* **188**, 73–86.

Favre J-F, Calmels TPG, Rouanet S, Javré J-L, Cheval B & Bril A (1999). Characterization of Kv4.3 in HEK 293 cells: comparison with the rate ventricular transient outward potassium current. *Cardiovasc Res* **41**, 188–199.

Fedida D, Braun AP & Giles WR (1993). Alpha-1 adrenoceptors in myocardium: functional aspects and transmembrane signaling mechanisms. *Physiol Rev* **73**, 469–487.

Fedida D & Giles WR (1991). Regional variations in action potentials and transient outward current in myocytes isolated from rabbit left ventricle. *J Physiol* **442**, 191–209.

Franqueza L, Valenzuela C, Eck J, Tamkun MM, Tamargo J & Snyders DJ (1999). Functional expression of an inactivating potassium channel (Kv4.3) in a mammalian cell line. *Cardiovasc Res* **41**, 212–219.

Gandhi CS & Isacoff EY (2002). Molecular models of voltage sensing. *J General Physiol* **120**, 455–463.

Gebauer M, Isbrandt D, Sauter K, Callsen B, Nolting A, Pongs O & Bähring R (2004). N-type inactivation features of Kv4.2 channel gating. *Biophys J* **56**, 210–223.

Giles W & Imaizumi Y (1988). Comparison of potassium currents in rabbit atrial and ventricular cells. *J Physiol* **405**, 123–145.

Glauner KS, Mannuzzu LM, Gandhi CS & Isacoff EY (1999). Spectroscopic mapping of voltage sensor movement in the Shaker potassium channel. *Nature* **402**, 813–817.

Greenstein JL, Wu R, Po S, Tomaselli GF & Winslow RL (2000). Role of the calcium-independent transient outward current I_{to1} in shaping action potential morphology and duration. *Circ Res* **87**, 1026–1033.

Gulbis JM, Mann S & MacKinnon R (1999). Structure of a voltage-dependent K^+ channel beta subunit. *Cell* **97**, 943–952.

Guo W, Xu H, London B & Nerbonne JM (1999). Molecular basis of transient outward K^+ current diversity in mouse ventricular myocytes. *J Physiol* **521**, 587–599.

Guo W, Li H, London B & Nerbonne JM (2000). Functional consequences of elimination of $I_{to,f}$ and $I_{to,s}$: early afterdepolarizations, atrioventricular block, and ventricular arrhythmia in mice lacking Kv1.4 and expressing a dominant-negative Kv4 alpha subunit. *Circ Res* **87**, 73–79.

Guo W, Li H, Aimond F, Johns DC, Rhodes KJ, Trimmer JS & Nerbonne JM (2002*a*). Role of heteromultimers in the generation of myocardial transient outward K^+ current. *Circ Res* **90**, 586–593.

Guo W, Malin SA, Johns DC, Jeromin A & Nerbonne JM (2002*b*). Modulation of Kv4-encoded K^+ currents in the mammalian myocardium by neuronal calcium sensor-1. *J Biol Chem* **277**, 26436–26443.

Gussack I & Antzelevitch C (2003). *Cardiac Repolarization.* Humana Press, Totowa, NJ, USA.

Han W, Bao W, Wang Z & Nattel S (2002*a*). Comparison of ion-channel subunit expression in canine cardiac Purkinje fibers and ventricular muscle. *Circ Res* **91**, 790–797.

Han W, Wang C & Nattel S (2000). A comparison of transient outward currents in canine cardiac Purkinje cells and ventricular myocytes. *Am J Physiol* **279**, H466–H474.

Han W, Zhang L, Schram G & Nattel S (2002*b*). Properties of potassium currents in Purkinje cells of failing human hearts. *Am J Physiol* **283**, H2495–H2503.

Hatano N, Ohya S, Muraki K, Clark RB, Giles WR & Imaizumi Y (2004). Two arginines in the cytoplasmic C-terminal domain are essential for voltage-dependent regulation o A-type K^+ current in the Kv4 channel subfamily. *J Biol Chem* **279**, 5450–5459.

Heginbotham L, Lu Z, Abramson T & MacKinnon R (1994). Mutations in the K^+ channel signature sequence. *Biophys J* **66**, 1061–1067.

Hille B (2001*a*). Gating mechanisms: kinetic thinking. *Ion Channels of Excitable Membranes*, 3rd edn, pp. 575–602. Sinauer Associates, Inc., Sunderland, MA, USA.

Hille B (2001*b*). Classic mechanisms of block. *Ion Channels of Excitable Membranes*, 3rd edn, pp. 503–537. Sinauer Associates, Inc., Sunderland, MA, USA.

Hodgkin AL & Huxley AF (1952). A quantitative description of membrane current and its application to conduction and excitation in nerve. *J Physiol* **117**, 500–544.

Holmqvist MH, Cao J, Hernandez-Pineda R, Jacobson MD, Carroll KI, Sung MA, Betty M, Ge P, Gilbride KJ, Brown ME, Jurman ME, Lawson D, Silos-Santiago I, Xie Y, Covarrubias M, Rhodes KJ, Distefano PS & An WF (2002). Elimination of fast inactivation in Kv4 A-type potassium channels by an auxiliary subunit domain. *Proc Natl Acad Sci U S A* **99**, 1035–1040.

Holmqvist MH, Cao J, Knoppers MH, Jurman ME, Distefano PS, Rhodes KJ, Xie Y & An WF (2001). Kinetic modulation of Kv4-mediated A-current by arachidonic acid is dependent on potassium channel interacting proteins. *J Neurosci* **21**, 4154–4161.

Hoshi T, Zagotta WN & Aldrich RW (1990). Biophysical and molecular mechanisms of Shaker potassium channel inactivation. *Science* **250**, 533–538.

Hoshi T, Zagotta WN & Aldrich RW (1991). Two types of inactivation in Shaker K^+ channels: effects of alterations in the carboxy-terminal region. *Neuron* **7**, 547–556.

Huelsing DJ, Spitzer KW & Pollard AE (2003). Spontaneous activity induced in rabbit Purkinje myocytes during coupling to a depolarized model cell. *Cardiovasc Res* **59**, 620–627.

Ikura M (1996). Calcium binding and conformational response in EF-hand proteins. *Trends Biochem Sci* **21**, 14–17.

Iyer V, Mazhari R & Winslow RL (2004). A computational model of the human left-ventricular epicardial myocyte. *Biophys J* **87**, 1507–1525.

Jerng HH & Corvarrubias M (1997). K^+ channel inactivation mediated by the concerted action of the cytoplasmic N- and C-terminal domains. *Biophys J* **72**, 163–174.

Jerng H, Qian Y & Pfaffinger PJ (2004). Modulation of Kv4.2 channel expression and gating by dipeptidyl peptidase 10 (DPP10). *Biophys J* **87**, 2380–2396.

Jerng HH, Shahidulla M & Corvarrubias M (1999). Inactivation gating of Kv4 potassium channels. Molecular interactions involving the inner vestibule of the pore. *J General Physiol* **113**, 641–660.

Jiang X, Bett GC, Li X, Bondarenko VE & Rasmusson RL (2003*a*). C-type inactivation involves a significant decrease in the intracellular aqueous Volume of Kv1.4 K^+ channels expressed in *Xenopus* oocytes. *J Physiol* **549**, 683–695.

Jiang Y, Lee A, Chen J, Ruta V, Cadene M, Chait BT & MacKinnon R (2003*b*). X-ray structure of a voltage-dependent K^+ channel. *Nature* **423**, 33–41.

Jiang Y, Ruta V, Chen J, Lee A & MacKinnon R (2003*c*). The principle of gating charge movement in a voltage-dependent K^+ channel. *Nature* **423**, 42–48.

Jiang QX, Wang DN & MacKinnon R (2004). Electron microscopic analysis of KvAP voltage-dependent K^+ channels in an open conformation. *Nature* **430**, 806–810.

Kääb S, Dixon J, Duc J, Ashen D, Näbaeur M, Beuckelmann DJ, Steinbeck G, McKinnon D & Tomaselli GF (1998). Molecular basis of transient outward potassium current down regulation in human heart failure: a decrease in Kv4.3 mRNA correlates with a reduction in current density. *Circulation* **98**, 1383–1393.

Kim LA, Furst J, Butler MH, Xu S, Grigorieff N & Goldstein SA (2003). Composition of I_{to} channels: Kv4.2-KChIP2 complexes carry four subunits of each type. *J Biol Chem* **279**, 5549–5554.

Kim LA, Furst J, Gutierrerz D, Butler MH, Xu S, Goldstein SA & Grigorieff N (2004). Three dimensional structure of I_{to}: Kv4.2-KChIP2 ion channels by electron microscopy at 21 Å resolution. *Neuron* **41**, 513–519.

Kuo H-C, Cheng C-F, Clark RB, Lin J, Gu Y, Ikeda Y, Chu P-H, Ross J, Giles WR & Chien KR (2001). A defect in the Kv channel-interacting protein 2 (KChIP2) gene leads to a complete loss of I_{to} and confers susceptibility to ventricular tachycardia. *Cell* **107**, 801–813.

Kuryshev YA, Gudz TI, Brown AM & Wible BA (2000). KChAP as a chaperone for specific K^+ channels. *Am J Physiol* **278**, C931–C941.

Laine M, Lin MA, Bannister JP, Silverman WR, Mock AF, Roux B & Papazian DM (2003). Atomic proximity between S4 segment and pore domain in Shaker potassium channels. *Neuron* **39**, 467–481.

Laine M, Papazian DM & Roux B (2004). Critical assessment of a proposed model of Shaker. *FEBS Lett* **564**, 257–263.

Larsson HP, Baker OS, Dhillon DS & Isacoff EY (1996). Transmembrane movement of the shaker K^+ channel S4. *Neuron* **16**, 387–397.

Lee S-Y & MacKinnon R (2004). A membrane access mechanism for ion channel inhibition by voltage sensor toxins from spider venom. *Nature* **430**, 232–235.

Li X, Bett GC, Jiang X, Bondarenko VE, Morales MJ & Rasmusson RL (2003). Regulation of N- and C-type inactivation of Kv1.4 by pH_o and K^+: evidence for transmembrane communication. *Am J Physiol* **284**, H71–H80.

Libbus I, Wan X & Rosenbaum DS (2004). Electrotonic load triggers remodeling of repolarizing current I_{to} in ventricle. *Am J Physiol* **286**, H1901–H1909.

Linse S & Forsén S (1995). Determinants that govern high-affinity calcium binding. In *Calcium Regulation of Cellular Function*, ed. Means AR, pp. 89–151. Raven Press, Ltd, New York.

Liu DW, Gintant GA & Antzelevitch C (1993). Ionic bases for electrophysiological distinctions among epicardial, midmyocardial and endocardial myocytes from the free wall of the canine left ventricle. *Circ Res* **72**, 671–687.

London B (2001). Cardiac arrhythmias: from (transgenic) mice to men. *J Cardiovasc Electrophysiol* **12**, 1089–1092.

London B, Wang DW, Hill JA & Bennet PB (1998*b*). The transient outward current in mice lacking the potassium channel gene Kv1.4. *J Physiol* **509**, 171–182.

McCormack T & McCormack K (1994). Shaker K^+ channel beta subunits belong to an NAD(P)H-dependent oxidoreductase superfamily. *Cell* **79**, 1133–1135.

McKinnon D (1999). Molecular identity of I_{to}: Kv1.4 redux. *Circ Res* **84**, 620–622.

MacKinnon R (2003). Potassium channels. *FEBS Lett* **555**, 62–65.

Mannuzzu LM, Moronne MM & Isacoff EY (1996). Direct physical measure of conformational rearrangement underlying potassium channel gating. *Science* **271**, 213–216.

Morales MJ, Castellino RC, Crews AL, Rasmusson RL & Strauss HC (1995). A novel β subunit increases rate of inactivation of specific voltage-gated channel α subunits. *J Biol Chem* **270**, 6272–6277.

Näbauer M, Beuckelmann DJ, Überfuhr P & Steinbeck G (1996). Regional differences in current density and rate-dependent properties of the transient outward current in subepicardial and subendocardial myocytes of human left ventricle. *Circulation* **93**, 168–177.

Nadal MS, Amarillo Y, de Miera EV & Rudy B (2001). Evidence for the presence of a novel Kv4-mediated A-type K^+ channel-modifying factor. *J Physiol* **537**, 801–809.

Nadal MS, Ozaita A, Amarillo Y, Vega-Saenz de Miera E, Vega-Saenz de Miera YE, Ma Y, Mo W, Goldberg EM, Misumi Y, Ikehara Y, Neubert TA & Rudy B (2003). The CD26-related dipeptidyl aminopeptidase-like protein DPPX is a critical component of neuronal A-type K^+ channels. *Neuron* **37**, 449–461.

Nakamura TY, Pountney DJ, Ozaita A, Nandi S, Ueda S, Rudy B & Coetzee WA (2001). A role for frequenin, a Ca^{2+}-binding protein, as a regulator of Kv4 K^+-currents. *Proc Natl Acad Sci U S A* **98**, 12808–12813.

Nef P (1996). Neuron specific calcium sensors (the NCS subfamily). In *Guidebook to the Calcium-Binding Proteins*, ed.Celio MR, Pauls T & Schwaller B, pp. 94–98. Oxford University Press, Oxford.

Nerbonne JM (2000). Molecular basis of functional voltage-gated K^+ channel diversity in the mammalian myocardium. *J Physiol* **525**, 285–298.

Nerbonne JM (2002). Molecular analysis of voltage-gated K^+ channel diversity and functioning in the mammalian heart. In *Handbook of Physiology*, section 2, *The Cardiovascular System*, vol. I, *The Heart*, ed. Page E, Fozzard HA & Solaro RJ, pp. 568–594. Oxford University Press, New York.

Nerbonne JM (2004). Studying cardiac arrhythmias in the mouse—a reasonable model for probing mechanisms? *Trends Cardiovas Med* **14**, 83–93.

Nerbonne JM & Kass RS (2003). Physiology and molecular biology of ion channels contributing to ventricular repolarization. In *Cardiac Repolarization*, ed. Gussack I & Antzelevitch C, pp. 25–62. Humana Press, Totowa, New Jersey.

Norton RS & Pallaghy PK (1998). The cysteine knot structure of ion channel toxins and related polypeptides. *Toxicon* **36**, 1573–1583.

Ohya S, Morohashi Y, Muraki K, Tomita T, Watanabe M, Iwatsubo T & Imaizumi Y (2001). Molecular cloning and expression of novel splice variants of K^+ channel interacting protein 2. *Biochem Biophys Res Com* **282**, 96–102.

Oudit GY, Kassiri Z, Sah R, Ramirez RJ, Zobel Z & Backx PH (2001). The molecular physiology of the cardiac transient outward potassium current (I_{to}) in normal and diseased myocardium. *J Mol Cell Cardiol* **33**, 851–872.

Parker C & Fedida D (2001). Cholinergic and adrenergic modulation of cardiac K^+ channels. In *Potassium Channels in Cardiovascular Biology*, ed. Archer SL & Rusch NJ, pp. 387–426. Kluwer Academic/Plenum Pubishers, New York.

Patel SP, Campbell DL & Strauss HC (2002*b*). Elucidating KChIP effects on Kv4.3 inactivation and recovery kinetics with a minimal KChIP2 isoform. *J Physiol 545* **1**, 5–11.

Patel SP, Campbell DL, Morales MJ & Strauss HC (2002*a*). Heterogeneous expression of KChIP2 isoforms in the ferret heart. *J Physiol* **539**, 649–656.

Patel SP, Parai R, Parai R & Campbell DL (2004). Regulation of Kv4.3 voltage-dependent gating kinetics by KChIP2 isoforms. *J Physiol* **557**, 19–41.

Patlak J (1991). Molecular kinetics of voltage-dependent Na^+ channels. *Physiol Rev* **71**, 1047–1080.

Perez-Garcia MT, López-López JR & Gonzalez C (1999). Kvβ1.2 subunit coexpression in HEK 293 cells confers O_2 sensitivity to Kv4.2 but not Shaker channels. *J General Physiol* **113**, 897–907.

Petersen KR & Nerbonne JM (1999). Expression environment determines K^+ current phenotypes: Kv1 and Kv4 α subunit-induced K^+ currents in mammalian cell lines and cardiac myocytes. *Pflugers Arch* **437**, 381–392.

Po S, Snyders DJ, Baker R, Tamkun MM & Bennet PB (1992). Functional expression of an inactivating potassium channel cloned from human heart. *Circ Res* **71**, 732–736.

Pourrier M, Herrera D, Caballero R, Schram G, Wang Z & Nattel S (2004). The Kv4.2 N-terminal restores fast inactivation and confers KChIP2 modulatory effects on N-terminal-deleted Kv1.4 channels. *Pflugers Arch* **449**, 235–247.

Puglisi JL & Bers DM (2001). LabHEART: an interactive computer model of rabbit ventricular myocyte ion channel and Ca transport. *Am J Physiol* **281**, C2049–C2060.

Puglisi JL, Wang F & Bers DM (2004). Modeling the isolated cardiac myocyte. *Prog Biophys Mol Biol* **85**, 28–38.

Rasmusson RL, Morales MJ, Castellino RC, Zhang Y, Campbell DL & Strauss HC (1995*a*). C-type inactivation controls recovery in a fast inactivating cardiac K^+ channel (Kv1.4) expressed in *Xenopus* oocytes. *J Physiol* **489**, 709–721.

Rasmusson RL, Morales MJ, Wang S, Liu S, Campbell DL, Brahmajothi MV & Strauss HC (1998). Inactivation of voltage-gated cardiac K^+ channels. *Circ Res* **20**, 739–750.

Rasmusson RL, Zhang Y, Campbell DL, Comer MB, Castellino RC, Liu S & Strauss HC (1995*b*). Bi-stable block by 4-aminopyridine of a transient K^+ channel (Kv1.4) cloned from ferret ventricle and expressed in *Xenopus* oocytes. *J Physiol* **485**, 59–71.

Ren X, Shand SH & Takimoto K (2003). Effective association of Kv channel-interacting proteins with Kv4 channel is mediated with their unique core peptide. *J Biol Chem* **278**, 43564–45570.

Robertson B (2001). Pharmacology of voltage-gated K^+ channels. In *Potassium Channels in Cardiovascular Biology*, ed. Archer SL & Rusch SJ, pp. 195–217. Kluwer Academic/Plenum Publishers, New York.

Roeper J, Lorra C & Pongs O (1997). Frequency-dependent inactivation of mammalian A-type K^+ channel Kv1.4 regulated by Ca^{2+}/calmodulin-dependent protein kinase. *J Neurosci* **17**, 3379–3391.

Rosati B, Grau F, Rodriguez S, Li H, Nerbonne JM & McKinnon D (2003). Concordant expression of KChIP2 mRNA, protein, and transient outward current throughout the canine ventricle. *J Physiol* **548**, 815–822.

Rosati B, Pan Z, Lypen S, Wang H-S, Cohen I, Dixon JE & McKinnon D (2001). Regulation of KChIP2 potassium channel β subunit gene expression underlies the gradient of transient outward current in canine and human ventricle. *J Physiol* **533**, 119–125.

Rudy Y (2002). The cardiac ventricular action potential. In *Handbook of Physiology*, section 2, *the Cardiovascular System*, vol. I, *The Heart*, ed. Page E, Fozzard H A & Solaro RJ, pp. 531–547. Oxford University Press, New York.

Ruppersberg JP, Frank R, Pongs O & Stocker M (1991*a*). Cloned neuronal IK_A channels reopen during recovery from inactivation. *Nature* **353**, 657–660.

Ruppersberg JP, Stocker M, Pongs O, Heinemann SH & Koenen M (1991*b*). Regulation of fast inactivation of cloned mammalian IK_A channels by cysteine oxidation. *Nature* **352**, 711–714.

Ruta V & MacKinnon R (2004). Localization of the voltage-sensor toxin receptor on KvAP. *Biochemistry* **43**, 10071–100079.

Sah R, Ramirez RJ, Oudit GY, Gidrewicz D, Triveri MG, Zobel C & Backx P (2003). Regulation of cardiac excitation-contraction coupling by action potential repolarization: role of the transient outward potassium current (I_{to}). *J Physiol* **546**, 5–18.

Sanguinetti MC & Bennett PB (2003). Antiarrhythmic drug target choices and screening. *Circ Res* **93**, 491–499.

Sanguinetti MC, Johnson JH, Hammerland LG, Kelbaugh PR, Volkmann RA, Saccomano NA & Mueller AL (1997). Heteropodatoxins: peptides isolated from spider venom that block Kv4.2 potassium channels. *Mol Pharmacol* **51**, 491–498.

Scannevin RH, Wang K-W, Jow F, Megules J, Kopsco DC, Edris W, Carroll KC, Lu Q, Xu W, Xu Z, Katz AH, Olland S, Lin L, Taylor M, Stahl M, Malakian K, Somers W, Mosyak L, Bowlby MR, Chandra P & Rhodes KJ (2004). Two N-terminal domains of Kv4 K^+ channels regulate binding to and modulation by KChIP1. *Neuron* **41**, 587–598.

Schönherr R, Manuzzu LM, Isacoff EY & Heinemann SH (2002). Conformational switch between slow and fast gating modes: allosteric regulation of voltage sensor mobility in the EAG K^+ channel. *Neuron* **35**, 935–949.

Schrader LA, Anderson AE, Mayne A, Pfaffinger PJ & Sweatt JD (2002). PKA modulation of Kv4.2-encoded A-type potassium channels requires formation of a supramolecular complex. *J Neurosci* **22**, 10123–10133.

Serodio P, Vega-Saenz DM & Rudy B (1996). Cloning of a novel component of A-type K^+ channels operating at subthreshold potentials with unique expression in heart and brain. *J Neurophysiol* **75**, 2174–2179.

Shahidullah M & Covarrubias M (2003). The link between ion permeation and inactivation gating of Kv4 potassium channels. *Biophys J* **84**, 928–941.

Shiau Y-S, Haung P-T, Liou H-H, Liaw Y-C, Shiau Y-Y & Lou K-L (2003). Structural basis of binding and inhibition of novel tarantula toxins in mammalian voltage-dependent potassium channels. *Chem Res Toxicol* **16**, 1217–1225.

Shimoni Y, Severson D & Giles W (1995). Thyroid status and diabetes modulate regional differences in potassium currents in rat ventricle. *J Physiol* **488**, 673–688.

Sokolova O (2004). Structure of cation channels, revealed by single particle electron microscopy. *FEBS Lett* **564**, 251–256.

Sokolova O, Kolmakova-Partensky L & Gigorieff N (2001). Three dimensional structure of a voltage-gated potassium channel at 2.5 nm resolution. *Structure* **9**, 215–220.

Starace DM & Bezanilla F (2001). Histidine scanning mutagenesis of basic residues of the S4 segment of the Shaker K^+ channel. *J General Physiol* **117**, 469–490.

Starace DM & Bezanilla F (2004). A proton pore in a potassium channel voltage sensor reveals a focused electric field. *Nature* **427**, 548–553.

Starace DM, Stefani E & Bezanilla F (1997). Voltage-dependent proton transport by the voltage sensor of the Shaker K^+ channel. *Neuron* **19**, 1319–1327.

Strauss HC, Morales MJ, Wang S, Brahmajothi MV & Campbell DL (2001). Voltage-dependent K^+ channels. In *Heart Physiology and Pathophysiology*, 4th edn, ed. Sperelakis N, Kurachi Y, Terzic A & Cohen MV, pp. 259–280. Academic Press, San Diego.

Strauss HC & Rasmusson RL (2002). Restitution, ventricular fibrillation, and drugs: where are we now? *J Cardiovas Electrophysiol* **13**, 915–917.

Swartz KJ & MacKinnon R (1997). Mapping the receptor site for Hanatoxin, a gating modifier of voltage-dependent K^+ channels. *Neuron* **18**, 675–682.

Taggart P, Sutton P, Opthof T, Coronel R & Kallis K (2003). Electrotonic cancellation of transmural electrical gradients in the left ventricle in man. *Prog Biophys Mol Bio* **82**, 243–254.

Tamkun M, Knoth KM, Walbridge M, Kroemer JA, Roden DM & Glover DM (1991). Molecular cloning and characterization of two voltage-gated K^+ channel cDNAs from human ventricle. *FASEB J* **5**, 331–337.

Tombola F, Pathak MM & Isacoff EY (2005). Voltage-sensing arginines in a potassium channel permeate and occlude cation-selective pores. *Neuron* **45**, 379–388.

Tseng GN, Jiang M & Yao JA (1996). Reverse use dependence of Kv4.2 blockade by 4-aminopyridine. *J Pharmacol Exp Ther* **279**, 865–876.

Tseng-Crank JCL, Tseng G-N, Schwartz A & Tanouye MA (1990). Molecular cloning and functional expression of a potassium channel cDNA isolated from a rat cardiac library. *FEBS Lett* **268**, 63–68.

Van Wagoner DR & Nerbonne JM (2001). Molecular mechanisms of atrial fibrillation. In *Heart Physiology and Pathophysiology*, 4th edn, ed. Sperelakis N, Kurachi Y, Terzic A & Cohen MV, pp. 1107–1124. Academic Press, San Diego.

Varro A, Lathrop DA, Hester SB, Nanasi PP & Papp JG (1993). Ionic currents and action potentials in rabbit, rat and guinea pig ventricular myocytes. *Basic Res Cardiol* **88**, 93–102.

Vega-Saenz de Miera E, Moreno H, Fruhling D, Kentros C & Rudy B (1992). Cloning of Sh III (Shaw-like) cDNAs encoding a novel high-voltage-activated, TEA-sensitive, type-A K^+ channel. *Proc Biol Sci* **248**, 9–18.

Verkerk AO & van Ginneken A (2001). Considerations when studying the transient outward K^+ current in cells exhibiting the hyperpolarization-activated current. *Cardiovascular Res* **52**, 517–518.

Wada K, Yokotani N, Hunter C, Doi K, Wenthold J & Shimaski S (1992). Differential expression of two distinct forms of mRNA encoding members of a depeptidyl aminopeptidase family. *Proc Natl Acad Sci U S A* **89**, 197–201.

Wang S, Bondarenko VE, Qu Y, Morales MJ, Rasmusson RL & Strauss HC (2004). Activation properties of Kv4.3 channels: time, voltage and $[K^+]_o$ dependence. *J Physiol* **557**, 105–717.

Wang S, Patel SP, Qu Y, Hua P, Strauss HC & Morales MJ (2002). Kinetic properties of Kv4.3 and their modulation by KChIP2b. *Biochem Biophys Res Comm* **295**, 223–229.

Wible BA, Yang Q, Kurysshev YA, Accili EA & Brown AM (1998). Cloning and expression of a novel K^+ channel regulatory protein, KChAP. *J Biol Chem* **273**, 11745–11751.

Wickenden AD, Lee P, Sah R, Huang Q, Fishman GI & Backx PH (1999). Targeted expression of a dominant-negative Kv4.2 K^+ channel subunit in the mouse heart. *Circ Res* **85**, 1067–1076.

Winslow RL, Contassa S & Greenstein JL (2005). Using models of the myocyte for functional interpretation of cardiac proteomic data. *J Physiol* **563**, 73–81.

Winslow RL, Scollan DF, Holmes A, Yung CK, Zhaang J & Jafri MS (2000). Electrophysiological modeling of cardiac ventricular function: from cell to organ. *Ann Rev Biomed Eng* **2**, 119–155.

Wissmann R, Bildl W, Oliver D, Beyermann M, Kalbitzer H-R, Bentrop D & Fakler B (2003). Solution structure and function of the 'tandem inactivation domain' of neuronal A-type potassium channel Kv1.4. *J Biol Chem* **278**, 16142–16150.

Xu H, Guo W & Nerbonne JM (1999). Four kinetically distinct depolarization-activated K^+ currents in adult mouse ventricular myocytes. *J General Physiol* **113**, 661–677.

Yang E-K, Alvira MR, Levitan ES & Takimoto K (2001). Kvβ subunits increase expression of Kv4.3 channels by interacting with their C termini. *J Biol Chem* **276**, 4839–4844.

Yellen G (1998). The moving parts of voltage-gated ion channels. *Quart Rev Biophys* **31**, 239–295.

Yellen G (2002). The voltage-gated potassium channels and their relatives. *Nature* **419**, 35–42.

Yeola SW & Snyders DJ (1997). Electrophysiological and pharmacological correspondence between Kv4.2 current and rat cardiac transient outward current. *Cardiovas Res* **33**, 540–547.

Zagotta WN, Hoshi T & Aldrich RW (1990). Restoration of inactivation in mutants of Shaker potassium channels by a peptide derived from ShB. *Science* **250**, 568–571.

Zhang M, Jiang M & Tseng GN (2001). MinK-related peptide associates with Kv4.2 and modulates its function: potential role as beta subunit of cardiac transient outward channel? *Circ Res* **88**, 1012–1019.

Zhou W, Qian Y, Kunjilar K, Pfaffinger PJ & Choe S (2004). Structural insights into the functional interaction of KChIP1 with Shal-type K^+ channels. *Neuron* **41**, 573–586.

Zicha S, Moss I, Allen B, Varro A, Papp J, Dumaine R, Antzelivitch C & Nattel S (2003). Molecular basis of species-specific expression of repolarizing K^+ currents in the heart. *Am J Physiol* **285**, H1641–H1649.

Zicha S, Xiao L, Stafford S, Cha TJ, Han W, Varro A & Nattel S (2004). Transmural expression of transient outward potassium current subunits in normal and failing canine and human hearts. *J Physiol* **561**, 735–748.

Acknowledgements

This work was supported by an American Heart Association Established Investigator Award to D.L.C.